

RESEARCH ARTICLE OPEN ACCESS

Functional Relationships of Two NFU Proteins in Maintaining the Abundances of Mitochondrial Iron–Sulfur Proteins

Jun Zhao^{1,2}  | Manasa B. Satyanarayan¹  | Joshua T. VanSlambrouck¹  | Alexander J. Kolstoe¹ | Michael J. Voyt¹  | Glory O. Jamesa¹ | Fei Yu²  | Yan Lu¹ 

¹Department of Biological Sciences, Western Michigan University, Kalamazoo, Michigan, USA | ²State Key Laboratory of Crop Stress Biology for Arid Areas and College of Life Sciences, Northwest A&F University, Yangling, Shaanxi, China

Correspondence: Yan Lu (yan.1.lu@wmich.edu)

Received: 18 September 2024 | **Revised:** 7 May 2025 | **Accepted:** 9 May 2025

Funding: This work was partially supported by the US National Science Foundation under Grant Numbers MCB-1244008, DBI-2146882, and DBI-2444114 (to Y. L.) and Western Michigan University (2021–2022 Faculty Research and Creative Activities Award Number 1627 to Y. L.).

Keywords: iron–sulfur carrier | Iron–sulfur cluster | mitochondrion | NFU4 | NFU5 | nitrogen-fixation-subunit-U (NFU)

ABSTRACT

Iron–sulfur clusters are involved in many biological processes, including photosynthetic electron transport in the chloroplast and respiratory electron transport in the mitochondrion. Iron–sulfur cluster biosynthesis requires iron–sulfur carriers such as nitrogen-fixation-subunit-U [NFU]-type proteins. The *Arabidopsis thaliana* nuclear genome encodes two mitochondrion-targeted NFU proteins: NFU4 and NFU5, previously reported to have a primary role in the biosynthesis of the lipoate cofactor, mediated by the 4Fe–4S enzyme lipoyl synthase. Through in vitro reconstitution and spectroscopic analysis, we found that recombinant NFU4 and NFU5 proteins had UV–visible features characteristic of 4Fe–4S clusters. In addition, we confirmed that double homozygous, complete loss-of-function *nfu4 nfu5* mutants had an embryo-lethal phenotype. To investigate the functional relationship between NFU4 and NFU5, we generated sesquimutants that were homozygous loss-of-function for one gene and heterozygous for the other, which appeared slightly smaller than *nfu4-2*, *nfu4-4*, and *nfu5-1* single mutants. This suggests that the simultaneous decrease in levels of NFU4 and NFU5 proteins may have an additive effect on plant growth. Quantitative reverse transcription PCR showed that the *NFU4* transcript was absent in mutants homozygous for *nfu4-2* and *nfu4-4* and that the *NFU5* transcript level was substantially reduced in the *nfu5-1* single mutant or sesquimutants. Consistent with the transcript data, the abundances of NFU4 and NFU5 proteins were either virtually absent or substantially reduced in the corresponding single mutants and sesquimutants. Immunoblot analysis showed that most *nfu4* and *nfu5-1* single, double, and sesquimutants had significant reductions in the levels of mitochondrial 4Fe–4S proteins, such as aconitase (ACO) and biotin synthase 2 (BIO2; note that BIO2 also contains a 2Fe–2S cluster). In addition, *nfu4 nfu5* sesquimutants showed substantial reductions in the protein level of the 75-kDa subunit of respiratory complex I (CI75), which contains one 2Fe–2S cluster and two 4Fe–4S clusters. These observations indicate that NFU4 and NFU5 are important in maintaining the levels of mitochondrial 4Fe–4S proteins. Such observations are also consistent with the hypothesis that NFU4 and NFU5 may serve as iron–sulfur carriers and may play a role in the transfer of 4Fe–4S clusters to recipient apoproteins, such as ACO and CI75, during the biogenesis and maturation of mitochondrial 4Fe–4S clusters.

This is an open access article under the terms of the [Creative Commons Attribution-NonCommercial-NoDerivs](https://creativecommons.org/licenses/by-nc-nd/4.0/) License, which permits use and distribution in any medium, provided the original work is properly cited, the use is non-commercial and no modifications or adaptations are made.

© 2025 The Author(s). *Plant Direct* published by American Society of Plant Biologists and the Society for Experimental Biology and John Wiley & Sons Ltd.

1 | Introduction

Iron–sulfur clusters participate in a variety of biological processes, such as respiratory electron transfer, photosynthetic electron transfer, oxidation–reduction reactions, and iron/sulfur storage (Beinert 2000; Johnson et al. 2005; Lill 2009; Przybyla-Toscano et al. 2021c). In plants, iron–sulfur clusters are best known for their roles in respiratory electron transport inside the mitochondrion and photosynthetic electron transport inside the chloroplast (Touraine et al. 2004; Balk and Lobréaux 2005; Johnson et al. 2005; Pilon et al. 2006; Balk and Pilon 2011; Couturier et al. 2013; Balk and Schaedler 2014; Lu 2018; Berger et al. 2020a; Berger et al. 2020b; Przybyla-Toscano et al. 2021b; Pedroletti et al. 2023; Kairis et al. 2024). Various types of iron–sulfur clusters are found in the mitochondrion, such as 2Fe–2S, 3Fe–4S, and 4Fe–4S (Przybyla-Toscano et al. 2021a; Przybyla-Toscano et al. 2021b; Pedroletti et al. 2023). Examples of mitochondrial iron–sulfur proteins include mitochondrial ferredoxin 1 (mFDX1) containing 2Fe–2S, glutamine oxoglutarate aminotransferase (GOGAT) containing 3Fe–4S, aconitase (ACO, a key enzyme in the tricarboxylic acid cycle) containing 4Fe–4S, biotin synthase 2 (BIO2) containing 2Fe–2S and 4Fe–4S, and 75-kDa respiratory complex I (NADH–ubiquinone oxidoreductase) protein CI75 containing 2Fe–2S and 4Fe–4S (Lill and Kispal 2000; Lill and Muhlenhoff 2008; Balk and Pilon 2011).

The biogenesis of 2Fe–2S and 4Fe–4S clusters in the higher plant mitochondrion is a four-step process (Braymer and Lill 2017; Przybyla-Toscano et al. 2021b; Pedroletti et al. 2023). The first step is the *de novo* assembly of 2Fe–2S clusters on the iron–sulfur cluster assembly scaffold-like proteins ISU1/2/3 by the nitrogen fixation 1 (NFS1) cysteine desulfurase (i.e., the sulfur donor) and an unknown iron donor (Léon et al. 2002; Léon et al. 2005; Busi et al. 2006; Xu and Møller 2006; Frazzon et al. 2007; Vazzola et al. 2007; Turowski et al. 2012; Armas et al. 2019; Armas et al. 2020; Fonseca et al. 2020; Fu et al. 2020; Caubrière et al. 2023). The second step is the transfer of newly assembled 2Fe–2S clusters from the ISU scaffold complex to either recipient apoproteins or the central glutaredoxin GRXS15 with the help from chaperone proteins and 2Fe–2S carrier proteins (Bandyopadhyay et al. 2008; Xu et al. 2009; Rouhier et al. 2010; Leaden et al. 2014; Couturier et al. 2015; Moseler et al. 2015; Leaden et al. 2016; Ivanova et al. 2019; Berndt et al. 2021; Moseler et al. 2021; Talib and Outten 2021; Li et al. 2022; López-López et al. 2022). The third step is the reductive fusion of two GRXS15-bound 2Fe–4S clusters into one 4Fe–4S cluster on the iron–sulfur cluster assembly 1 and 2 (ISCA1–ISCA2) heterodimer (Zannini et al. 2018; Azam et al. 2020b; Weiler et al. 2020). The fourth step is the transfer of newly assembled 4Fe–4S clusters from the ISCA1–ISCA2 heterodimer to recipient apoproteins with the help from iron–sulfur carrier proteins (Waller et al. 2010; Waller et al. 2012; Wydro et al. 2013; Couturier et al. 2014; Uzarska et al. 2018; Azam et al. 2020a), such as nitrogen-fixation-subunit-U (NFU)-type proteins. NFU-type proteins exist ubiquitously in eukaryotes and nitrogen-fixing prokaryotes (Léon et al. 2003; Lill 2009). In the higher plant *Arabidopsis thaliana*, there are two nuclear-encoded mitochondrion-targeted NFU proteins: NFU4 and NFU5 (Léon et al. 2003; Yabe et al. 2004; Przybyla-Toscano et al. 2018; Przybyla-Toscano et al. 2021b). Full-length NFU4 and NFU5 contain a mitochondrial transit peptide, an N-terminal domain,

and a redox-active NFU domain with a conserved iron–sulfur-binding CXXC motif (C stands for cysteine and X stands for any amino acid) (Léon et al. 2003; Yabe et al. 2004; Przybyla-Toscano et al. 2018; Touraine et al. 2019). The mitochondrial localization of NFU4 and NFU5 had been demonstrated by fluorescent protein tagging and confocal microscopic analysis (Léon et al. 2003; Przybyla-Toscano et al. 2022).

NFU4 and NFU5 were previously proposed to participate in the biogenesis of mitochondrial 4Fe–4S clusters (Azam et al. 2020a; Przybyla-Toscano et al. 2022). Azam et al. (2020a) provided *in vitro* data that the 4Fe–4S cluster bound to recombinant NFU4 and NFU5 proteins can serve as the donor for the maturation of ACO2, a mitochondrial protein containing 4Fe–4S. Przybyla-Toscano et al. (2022) found that NFU4 and NFU5 interact with mitochondrial lipoyl synthase LIP1, which contains two 4Fe–4S clusters, in yeast-two-hybrid and bimolecular fluorescence complementation assays. Przybyla-Toscano et al. (2022) also provided *in planta* data that loss-of-function mutations in the *NFU4* and *NFU5* genes result in decreased protein lipoylation. Therefore, we hypothesize that NFU4 and NFU5 may serve as iron–sulfur carriers during the biogenesis of 4Fe–4S clusters in the mitochondria.

In this work, we investigated the role of and the relationship between the two mitochondrion-targeted NFU proteins in *Arabidopsis*. Through spectroscopic analysis, we found that recombinant NFU4 and NFU5 proteins possessed features characteristic of 4Fe–4S clusters. *In vitro* reconstitution assays showed that NFU4 and NFU5 may have an iron–sulfur scaffold function. It was previously reported that double homozygous *nfu4 nfu5-1* mutants had an embryo-lethal phenotype (Przybyla-Toscano et al. 2022; Wang 2022). Because of the lack of viable, complete loss-of-function *nfu4^{-/-} nfu5^{-/-}* double mutants, we analyzed the phenotypes, *NFU4/5* transcript levels, *NFU4/5* protein abundances, and other iron–sulfur protein contents in *nfu4-2/4^{-/-} nfu5-1^{+/-}* and *nfu4-2/4^{+/-} nfu5-1^{-/-}* sesquimutants. We found that the levels of 4Fe–4S protein ACO and 2Fe–2S and 4Fe–4S proteins BIO2 and CI75 were significantly reduced in the four sesquimutants. On the contrary, the level of 2Fe–2S protein mFDX1 was relatively uniform across the 10 different genotypes. These observations indicate that NFU4 and NFU5 are important in maintaining the levels of mitochondrial 4Fe–4S proteins. These results are also consistent with the hypothesis that NFU4 and NFU5 may serve as iron–sulfur carriers during mitochondrial 4Fe–4S biosynthesis and may play a role in the transfer of 4Fe–4S clusters to recipient apoproteins, during the maturation of mitochondrial proteins containing 4Fe–4S (Azam et al. 2020a).

2 | Materials and Methods

2.1 | Plant Materials and Growth Conditions

Arabidopsis (*A. thaliana*) T-DNA insertion lines *nfu4-2*, *nfu4-3*, *nfu4-4*, *nfu5-1*, and *nfu5-3* used in this study were obtained from the *Arabidopsis* Biological Resource Center (stock numbers SALK_061018, SAIL_590_F04, SAIL_1233_C08, WiscDsLoxHs069_06B, and GT_3_2834, respectively). The *nfu4-2*, *nfu4-3*, *nfu4-4*, and *nfu5-1* mutants are in the Columbia

(Col) ecotype (Alonso et al. 2003; Woody et al. 2007). The *nfu5-3* mutant (GT_3_2834) is in the Landsberg erecta (Ler) ecotype (Pan et al. 2003), which is morphologically different from Col. Therefore, *nfu5-3* was only used to create sesquimutant plants for seed segregation analysis. Mutant genotypes were confirmed by PCR, using Phire Plant Direct PCR kits (Thermo Scientific) and genotyping primers listed in Table S1 (Satyanarayan et al. 2021). Plants were grown in a growth chamber on a 12-h light/12-h dark photoperiod. The daytime light intensity was $150\ \mu\text{mol photons m}^{-2}\text{s}^{-1}$, the temperature was 20°C , and the relative humidity was 50% (Nath et al. 2017; Satyanarayan et al. 2021). Mature rosette leaves of 4-week-old plants were used for fresh weight measurements and extractions of pigments, RNA, and total proteins, unless stated otherwise.

2.2 | Expression and Purification of Recombinant NFU4 and NFU5 Proteins

Expression and purification of recombinant NFU4 and NFU5 proteins in *Escherichia coli* was performed as described previously (Clark and Lu 2015; Nath et al. 2016; Hackett et al. 2017; Satyanarayan et al. 2021). Total leaf RNA was extracted from a Col wild-type *Arabidopsis* plant, digested with RNase-free DNase I, and reverse-transcribed with oligo (dT)₁₅ primers and Moloney murine leukemia virus reverse transcriptase. Full-length *NFU4* and *NFU5* cDNAs (*NFU4*^{1–852} bp, corresponding to *NFU4*^{1–283} AA; *NFU5*^{1–828} bp, corresponding to *NFU5*^{1–275} AA), as well as *NFU4* and *NFU5* cDNAs lacking the mitochondrial transit peptide (*NFU4*^{163–852} bp, corresponding to *NFU4*^{55–283} AA; *NFU5*^{229–828} bp, corresponding to *NFU5*^{77–275} AA) were amplified using the mRNA:cDNA hybrid; phusion high-fidelity DNA polymerase (New England Biolabs); forward primers *NFU4*_BamH1_ATG, *NFU5*_BamH1_ATG, *NFU4*_BamH1_noTP, and *NFU5*_BamH1_noTP2; and reverse primers *NFU4*_Xho1_TAG and *NFU5*_Xho1_TAG (Table S1). The resulting PCR products were AT cloned into the pGEM-T Easy Vector (Promega) and sequenced to confirm the absence of PCR errors. BamH1/Xho1-digested fragments were subcloned into the pET28a expression vector (Novagen) and were expressed in *E. coli* strain Rosetta 2 (DE3) (Novagen). Overnight cultures of Rosetta 2 (DE3) harboring the *NFU4*^{163–852} bp and *NFU5*^{229–828} bp genes were diluted 1:20 and grown at 37°C for 1 h. Expression of the recombinant *NFU4*^{55–283} AA and *NFU5*^{77–275} AA proteins was induced with 1-mM isopropyl b-D-thiogalactoside, and cells were grown at 28°C overnight. The recombinant proteins were affinity purified with nickel-nitrilotriacetic acid (Ni-NTA) agarose under native and aerobic conditions according to the QIAexpressionist protocol (QIAGEN).

2.3 | Absorption Spectra of the As-Purified, Reduced, and Reconstituted Recombinant NFU4 and NFU5 Proteins

Absorption spectroscopy of the recombinant *NFU4*^{55–283} AA and *NFU5*^{77–275} AA proteins was carried out as described previously (Nakamaru-Ogiso et al. 2002; Yabe and Nakai 2006; Schwenkert et al. 2010; Nath et al. 2016; Satyanarayan et al. 2021). The absorption spectra (300–700 nm) of the purified recombinant proteins were recorded on a BioMate 3S spectrophotometer

(Thermo Scientific) before and after treating the proteins with 10-mM sodium dithionite, a reducing agent capable of reducing iron–sulfur clusters. In vitro reconstitution of iron–sulfur clusters on the recombinant proteins was performed in a Bactron anaerobic chamber. The as-purified recombinant proteins were incubated in 100- μM ammonium ferrous sulfate and 100- μM sodium sulfide at 25°C for 2 h in degassed buffer containing 50-mM Tris-HCl (pH 7.5), 50-mM NaCl, and 5-mM dithiothreitol. This is followed by a desalting step using an illustra NAP-10 column (GE Healthcare Life Sciences), and the absorption spectra of the reconstituted recombinant proteins were recorded.

2.4 | Fresh Weight Measurements

The fresh weights of the above-ground portions of 4-week-old plants (four different plants per genotype) were determined with an analytical balance, as described previously (de Ollas et al. 2019; Satyanarayan et al. 2021).

2.5 | Measurement of Chlorophyll and Carotenoid Contents

Chlorophyll and carotenoid were extracted from mature rosette leaves of 4-week-old plants (four independent pigment extractions from different plants for each genotype) with 80% acetone in 2.5-mM HEPES-KOH, pH 7.5, and the contents (mg) of total chlorophyll and carotenoid per gram of fresh tissues were determined on a BioMate 3S spectrophotometer (Thermo Scientific) as described previously by Wellburn (1994).

2.6 | Quantitative RT-PCR

Quantitative RT-PCR was performed as previously described (Nath et al. 2016; Hackett et al. 2017), with minor modifications. Total RNA was extracted from mature rosette leaves of 4-week-old plants (six independent RNA extractions from different plants for each genotype), using the RNeasy plant mini kit (QIAGEN), digested with RNase-free DNase I (QIAGEN), and reverse transcribed with oligo (dT)₁₅ primers (Promega) and Moloney murine leukemia virus reverse transcriptase (Promega) to generate the mRNA:cDNA hybrids. Quantitative PCR was performed on a StepOnePlus real-time PCR System (Thermo Fisher) with the mRNA:cDNA hybrids, Power SYBR Green PCR master mix (Thermo Fisher), and quantitative RT-PCR primers listed in Table S1. *ACTIN2* (At3g18780) was used as an internal reference for normalization. The average ratio of *NFU4* or *NFU5* transcripts to the *ACTIN2* transcript was normalized to 1.0 in the Col wild type.

2.7 | Extraction of Total Leaf Proteins

Total proteins were extracted from mature rosette leaves of 4-week-old plants (three to four independent protein extractions from different plants for each genotype) as previously described (Hackett et al. 2017; Satyanarayan et al. 2021). Approximately ~100 mg of mature rosette leaves were excised, frozen in liquid nitrogen, and then ground into fine powder

with stainless steel beads and TissueLyser II (Qiagen). Freshly prepared plant protein extraction buffer (50-mM Tris-HCl, pH 7.5, 150-mM NaCl, 1% Triton X-100, 0.5% sodium deoxycholate, 0.1% SDS, 1-mM EDTA, 1-mM DTT, and 1% of plant protease inhibitor cocktail [Sigma P9599-5ML]) was added to the frozen powder at 5 μ L/mg tissues. The samples were further homogenized with TissueLyser II. The homogenates were centrifuged at >10,000g and 4°C for 3 min. The resulting supernatants were transferred to a new set of microfuge tubes and centrifuged again at >10,000g and 4°C for 3 min to remove residual tissues. The total protein concentrations were then determined using the detergent-compatible (DC) protein assay (Bio-Rad 5,000,112) with 0–1.4 mg/mL of bovine serum albumin as standards.

2.8 | SDS-PAGE and Immunoblot Analysis

SDS-PAGE and immunoblot analyses of total leaf proteins were carried out as previously reported (Hackett et al. 2017; Satyanarayan et al. 2021), with minor modifications. Total leaf proteins from 4-week-old plants (three to four independent protein extractions from different plants for each genotype) were loaded on an equal total protein basis in amounts within the detection range. Proteins were then separated with SDS-PAGE (4%–20% polyacrylamide gels for NFU4 and NFU5 proteins; 10% polyacrylamide gels for other proteins), using the Mini PROTEAN Tetra Cell vertical gel electrophoresis system (Bio-Rad). After electrophoresis, the proteins were transferred to polyvinylidene difluoride membranes (EMD Millipore) using the Trans-Blot electrophoresis transfer cell (Bio-Rad). The membranes were sequentially incubated in a blocking solution (5% nonfat dry milk and 0.1% Tween-20 in 1X Tris buffered saline), a diluted primary antibody solution, and then a freshly prepared secondary antibody solution. The mitochondrial protein methylcrotononyl-CoA carboxylase 1 (MCCC1, i.e., the alpha subunit of the enzyme) does not contain any iron–sulfur (Fe–S) clusters and was used as the immunoblotting control. Rubisco large subunit (RbcL) stained with Coomassie Brilliant Blue was used as the loading control. The anti-NFU4 and anti-NFU4/5 (originally named anti-NFU5) antibodies were gifts from Dr. Nicolas Rouhier at Université de Lorraine (Przybyla-Toscano et al. 2022). The anti-NFU4/5 antibody reacts with both NFU4 and NFU5 (Przybyla-Toscano et al. 2022). All other primary antibodies were purchased from Agrisera, PhytoAB, or Sigma (mFDX1, #AS06 121, 1:1000 dilution; GOGAT, #AS07 242, 1:2000 dilution; ACO, #AS09 521, 1:10,000 dilution; CI75, PhytoAB #PHY1084S, 1:2000 dilution; BIO2, PhytoAB #PHY1815A, 1:2000; and MCCC1, Sigma #WH0056922M1-100UG, 1:2000 dilution). The anti-MCCC1 antibody was raised in mice, and all other primary antibodies were raised in rabbits. If the primary antibody was raised in rabbits, a horseradish peroxidase (HRP)-conjugate goat-anti-rabbit IgG antibody (Thermo Fisher Scientific #31460, 1:10,000 dilution) was used as the secondary antibody. If the primary antibody was raised in mice, a horseradish peroxidase (HRP)-conjugate goat-anti-mouse IgG antibody (Thermo Fisher Scientific #31430, 1:10,000 dilution) was used as the secondary antibody. Immunodetection of proteins on the polyvinylidene difluoride membrane was performed using the SuperSignal West Pico mouse or rabbit

IgG-detecting kit (Thermo Fisher) and analyzed by the Gel Logic 1500 Imaging System (Kodak). The quality of each immunoblot was inspected with the Carestream Molecular Imaging Software to make sure that band intensities were well within the detection range. Immunoblots with saturated signals were discarded and re-performed with reduced amounts of total proteins. Immunoblots with overly weak signals were also discarded and re-performed with increased amounts of total proteins. Densitometric analysis was performed with the Multi Gauge V3.0 software (Fujifilm Life Science). The average signal intensity of each protein was normalized to 1.0 in the Col wild type.

2.9 | Statistical Analysis

Mean value calculations, standard error calculations, and graphing were done in Microsoft Excel. Pairwise Student's *t*-test and correlation analysis were performed with JMP Pro 18.0.2 statistical software (SAS Institute). Levels of correlations were defined according to the correlation coefficient (*r*) values: 0.00–0.19 (0.00 to –0.19), very weak positive (negative); 0.20–0.39 (–0.20 to –0.39), weak positive (negative); 0.40–0.59 (–0.40 to –0.59), moderate positive (negative); 0.60–0.79 (–0.60 to –0.79), strong positive (negative); and 0.80–1.00 (–0.80 to –1.00), very strong positive (negative) (Meghanathan 2016). Detailed information about replicate numbers and statistical tests are provided in figure legends.

3 | Results

3.1 | Absorption Spectra of Recombinant NFU4 and NFU5 Showed Features of 4Fe–4S Clusters

The *NFU4* and *NFU5* genes are predicted to encode a 283-amino acid (AA) protein and a 275-AA protein, respectively (Figure 1a). As described previously, the full-length coding region of *NFU4* includes a mitochondrial transit peptide (1–54 AAs), an N-terminal domain (82–168 AAs), and a redox-active NFU domain (196–264 AAs) with the conserved CXXC motif at the C-terminus (Figure 1a). Similarly, the full-length coding region of *NFU5* includes a mitochondrial transit peptide (1–76 AAs), an N-terminal domain (77–163 AAs), and a redox-active NFU domain (191–259 AAs) with the conserved CXXC motif (Figure 1a). Green fluorescent protein tagging, confocal microscopic analysis, and quantitative mitochondrial proteomics showed that *NFU4* and *NFU5* are targeted to the mitochondrion (Léon et al. 2003; Fuchs et al. 2020; Przybyla-Toscano et al. 2022). *NFU4* and *NFU5* were proposed to participate in the biogenesis of mitochondrial 4Fe–4S clusters (Azam et al. 2020a; Przybyla-Toscano et al. 2022). Therefore, we expressed 6xHis-tagged *NFU4* and *NFU5* proteins in *E. coli* strain Rosetta 2 (DE3) and purified the recombinant proteins with nickel-charged agarose resin under native and aerobic conditions. To ensure protein solubility, the mitochondrial transit peptide in *NFU4* and *NFU5* was removed to produce *NFU4*^{55–283 AA} and *NFU5*^{77–275 AA}, respectively. The absorption spectra of the as-purified *NFU4*^{55–283 AA} and *NFU5*^{77–275 AA} proteins each had a broad absorption peak around 410 nm (Figure 1b,c), a signature feature of 4Fe–4S clusters (Kennedy

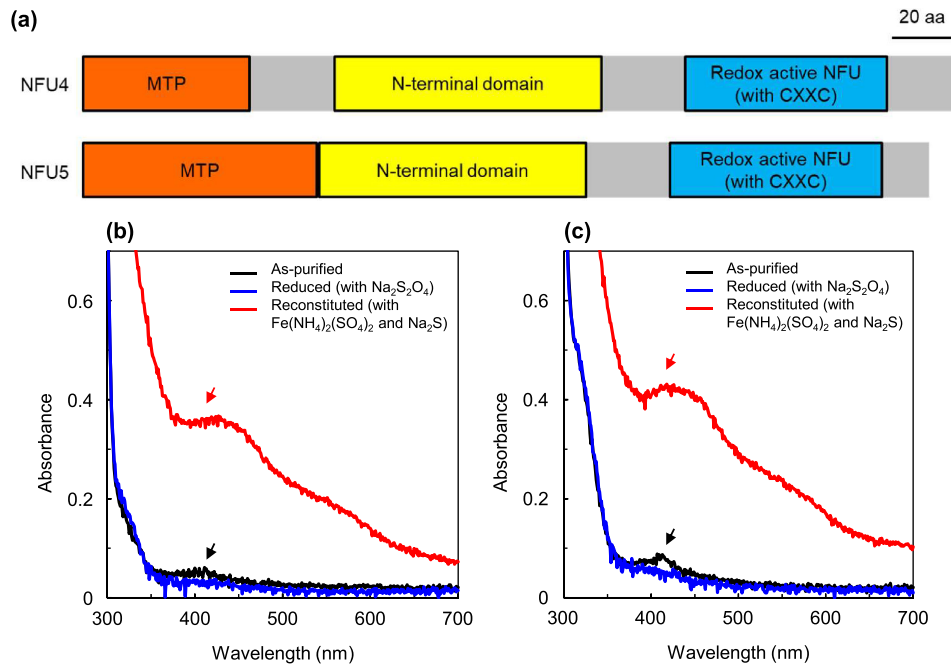


FIGURE 1 | Domain composition and absorption spectra of as-purified, reduced, and reconstituted recombinant NFU4 and NFU5 proteins. (a) Domains in full-length NFU4 and NFU5 proteins. Orange boxes represent the mitochondrial transit peptide; yellow boxes represent the N-terminal domain unique to mitochondrial-targeted NFU proteins; cyan boxes represent the redox-active NFU domain with the conserved CXXC motif. (b–c) Absorption spectra of as-purified, reduced, and reconstituted recombinant NFU4 (b) and NFU5 (c) proteins. Recombinant NFU4^{55–283 AA} and NFU5^{77–275 AA} were purified aerobically, and an absorption spectrum was recorded (black line). The blue curve represents the absorption spectrum of recombinant NFU4 and NFU5 proteins after reduction with 10-mM sodium dithionite. The black and red arrow points to the absorption peak at 410 nm, a typical feature of 4Fe–4S clusters, which disappears upon reduction by 10-mM sodium dithionite. The red curve represents the absorption spectrum of the recombinant proteins after reconstitution with ammonium ferrous sulfate and sodium sulfide. aa, amino acids.

et al. 1984; Nakamaru-Ogiso et al. 2002), which is consistent with the proposed role of NFU4 and NFU5 in the biogenesis of mitochondrial 4Fe–4S clusters.

3.2 | In Vitro Reconstitution Indicated an Iron–Sulfur Scaffold Function of NFU4 and NFU5

The 410-nm broad absorption peak of the as-purified NFU4^{55–283 AA} and NFU5^{77–275 AA} proteins disappeared after the addition of 10 -mM reducing agent sodium dithionite (Figure 1b,c). This suggests that iron–sulfur clusters bound to the as-purified NFU4 and NFU5 proteins are redox sensitive (Nakamaru-Ogiso et al. 2002). To test whether NFU4 and NFU5 have an iron–sulfur scaffold function, we performed in vitro reconstitution of iron–sulfur clusters on the recombinant NFU4 and NFU5 proteins, by treating the protein with an equimolar content of ferrous ion and sulfide. The 410-nm absorption peak became more evident after this treatment (Figure 1b,c). These experiments suggested that NFU4 and NFU5 may have an iron–sulfur scaffold function, especially toward 4Fe–4S clusters.

3.3 | Phenotypic Characterization of *nfu4* and *nfu5* Single, Double, and Sesquimutants

To investigate the in vivo function of NFU4 and NFU5 proteins, we obtained loss-of-function *nfu4* and *nfu5* T-DNA insertion mutants in *Arabidopsis* (Figure 2). The *nfu4-2*, *nfu4-3*,

and *nfu4-4* mutants have a T-DNA inserted in the first intron, the 100-nucleotide 5′-untranslated region (UTR), and the third intron, respectively (Figure 2a). The *nfu5-1* and *nfu5-3* mutants have a T-DNA inserted in the second intron and the second exon, respectively (Figure 2a). T-DNA insertion lines *nfu4-2*, *nfu4-4*, and *nfu5-1* have been previously validated as knockout lines, and *nfu5-3* has been validated as a knockdown line (Przybyla-Toscano et al. 2022). As mentioned in Materials and Methods, the *nfu4-2*, *nfu4-4*, and *nfu5-1* mutants are in the Col ecotype whereas the *nfu5-3* mutant is in the Ler ecotype (Figure 2a). Because of the morphological differences between the Col and Ler ecotypes, *nfu5-3* was only used to create sesquimutant plants for seed segregation analysis (see Figure 3). To study the functional relationship between NFU4 and NFU5, we attempted to generate double homozygous *nfu4 nfu5* mutants. We were able to generate the double homozygous *nfu4-3 nfu5-1* mutant (Figure 2b), because *nfu4-3* has the T-DNA inserted in the 100-nucleotide 5′-UTR of the *NFU4* gene (Figure 2a). However, our attempts to generate double homozygous *nfu4-2/4 nfu5-1/3* mutants were unsuccessful. For example, approximately one-fourth of fertilized ovules from the *nfu4-2/4^{-/-} nfu5-1/3^{+/-}* plants did not develop into normal seeds (Figure 3). This observation is consistent with the previous report that double homozygous *nfu4-2/4 nfu5-1* mutants had an embryo-lethal phenotype (Przybyla-Toscano et al. 2022).

Because of the lack of viable, complete loss-of-function *nfu4^{-/-} nfu5^{-/-}* double mutants, it was challenging to investigate the functional relationship between NFU4 and NFU5. To

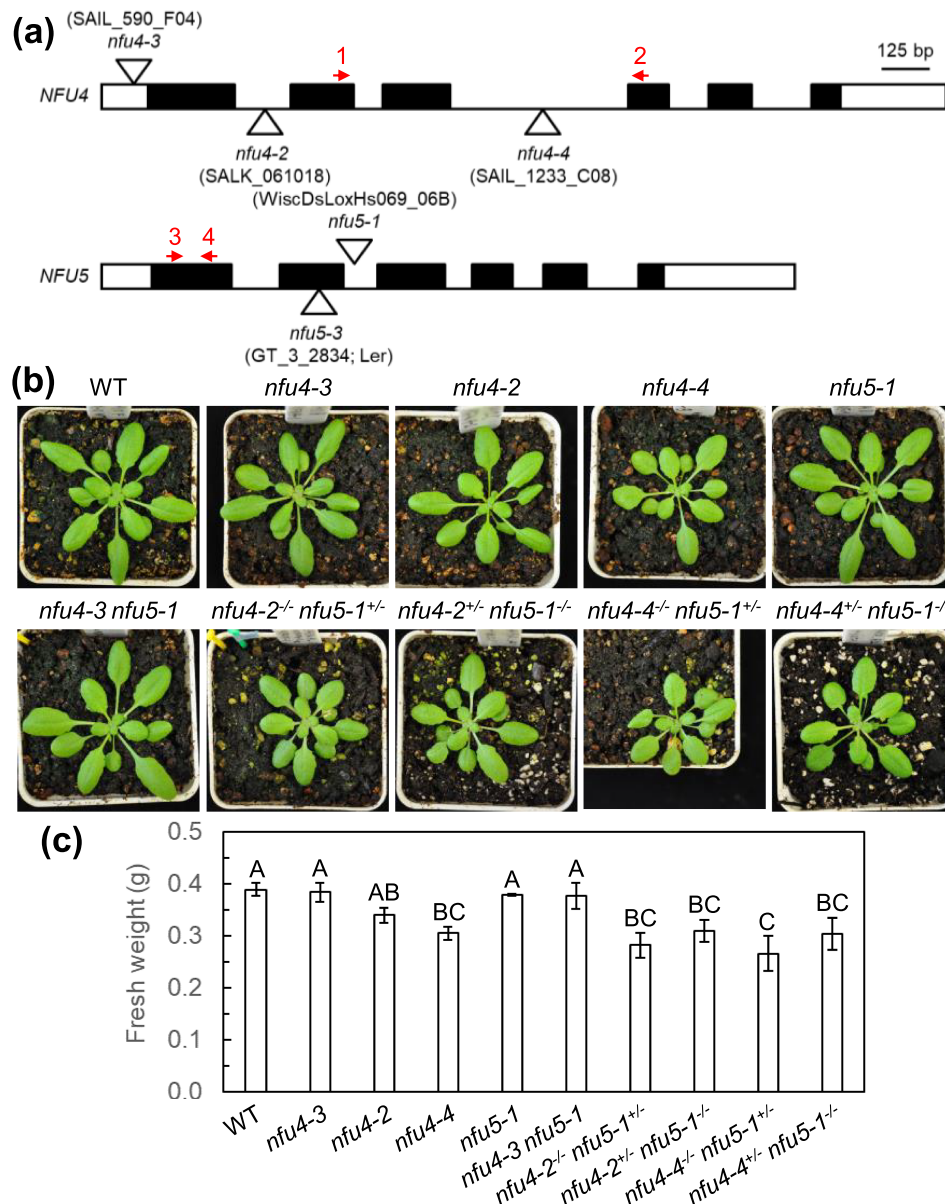


FIGURE 2 | Phenotype of *nfu4* and *nfu5-1* single, double, and sesquimutants. (a) Structure of *NFU4* and *NFU5* genes and locations of *nfu4* and *nfu5* mutations. White boxes, untranslated regions; black boxes, exons; lines, introns; and triangles, T-DNA insertions. Red arrows 1 and 2, left and right qRT-PCR primers for *NFU4*; red arrows 3 and 4, left and right qRT-PCR primers for *NFU5*. The *nfu4-2*, *nfu4-3*, *nfu4-4*, and *nfu5-1* mutants are in the Columbia (Col) background. The *nfu5-3* mutant is in the Landsberg erecta (Ler) background, which is morphologically different from Col. Therefore, *nfu5-3* was only used to create sesquimutant plants for seed segregation analysis. (b) Images of 4-week-old plants grown on a 12-h light/12-h dark photoperiod with an irradiance of 150- $\mu\text{mol photons m}^{-2}\text{s}^{-1}$ during the light period. (c) Above-ground fresh weight of 4-week-old plants. Values are presented as mean \pm SE ($n=4$ individual plants/genotype). Values not connected by the same uppercase letter are significantly different (Student's *t*-test, $p < 0.05$). bp, base pair; WT, wild type.

overcome this problem, we isolated the *nfu4-2^{-/-}* (homozygous) *nfu5-1^{+/-}* (heterozygous), *nfu4-2^{+/-} nfu5-1^{-/-}*, *nfu4-4^{-/-} nfu5-1^{+/-}*, and *nfu4-4^{+/-} nfu5-1^{-/-}* sesquimutants (Figure 2b). We crossed homozygous *nfu4-2* and *nfu4-4* mutants with the homozygous *nfu5-1* mutant. The resulting F_1 populations were screened for double heterozygous *nfu4 nfu5-1* mutants. Genotyping was performed by amplifying DNA from 2-week-old seedlings, using the Phire Plant Direct PCR kit (Thermo Scientific) and genotyping primers listed in Table S1. The self-fertilized segregating F_2 seeds were harvested from double heterozygous *nfu4 nfu5-1* plants and were then sown on soil. The resulting F_2 seedlings were genotyped to screen for sesquimutants. The genotype of

each sesquimutant plant was carefully confirmed, prior to plant imaging or tissue harvesting.

As shown in Figure 2b, *nfu4-2/4^{-/-} nfu5-1^{+/-}* and *nfu4-2/4^{+/-} nfu5-1^{-/-}* sesquimutants appeared slightly smaller than the Col wild type and the respective single mutants at the same age (4-week-old). Consistent with this visual observation, the fresh weight of the *nfu4-2^{-/-} nfu5-1^{+/-}* sesquimutant was significantly (~27%) lighter than the Col wild type and the *nfu5-1* single mutant at the same age (4-week-old) and slightly (~17%) lighter than the *nfu4-2* single mutant at the same age (Figure 2c). Similarly, the fresh weight of the *nfu4-4^{-/-} nfu5-1^{+/-}* sesquimutant was

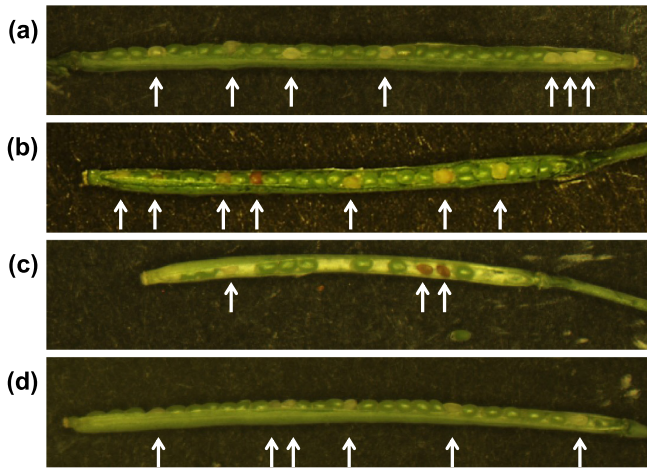


FIGURE 3 | Representative siliques from *nfu4-2/4^{-/-} nfu5-1/3^{+/-}* plants. (a–d) Siliques from (a) *nfu4-2^{-/-} nfu5-1^{+/-}*, (b) *nfu4-2^{-/-} nfu5-3^{+/-}*, (c) *nfu4-4^{-/-} nfu5-1^{+/-}*, and (d) *nfu4-4^{-/-} nfu5-3^{+/-}* plants. In (a), seven of the 32 seeds in this silique were aborted. In (b), seven of the 27 seeds in this silique were aborted. In (c), three of the 12 seeds in this silique were aborted. In (d), six of the 28 seeds were aborted. White arrows indicate aborted seeds.

significantly (~31%) lighter than those of the Col wild type and the *nfu5-1* single mutant and slightly (~13%) lighter than that of the *nfu4-4* single mutant (Figure 2c). These observations are in agreement with the sizes of the Col wild type, *nfu4-2 nfu5-1/nfu5-2* hemizygous mutant, and *nfu4-2 nfu5-2* double mutant grown under standard conditions by Przybyla-Toscano et al. (2022). According to Przybyla-Toscano et al. (2022), the *nfu5-2* mutant has the T-DNA inserted in the promoter region (251 nucleotides upstream of ATG). When Przybyla-Toscano et al. (2022) grew the same genotypes for normal (380 ppm) and low (150 ppm) CO₂ treatments, the slightly small phenotype of the *nfu4-2 nfu5-1/nfu5-2* hemizygous mutant disappeared. Such slight discrepancies in plant sizes might be due to the differences in growth conditions.

3.4 | Chlorophyll and Carotenoid Contents Are Reduced in *nfu4-2/4^{-/-} nfu5-1^{+/-}* and *nfu4-2/4^{+/-} nfu5-1^{-/-}* Sesquimutants

We also determined the amounts of chlorophyll *a*, chlorophyll *b*, carotenoid, and total chlorophyll in mature rosette leaves of 4-week-old plants (Figure 4). The amounts of these pigments in the *nfu4-2* single mutant were similar to those in the Col wild type (Figure 4a–d). However, the *nfu4-4* single mutant appeared to have ~15% lower levels of chlorophyll *a*, chlorophyll *b*, carotenoid, and total chlorophyll than the Col wild type (Figure 4a–d), possibly due to allelic differences between *nfu4-2* and *nfu4-4*. We found that the amounts of these pigments in *nfu4-2^{-/-} nfu5-1^{+/-}* and *nfu4-2^{+/-} nfu5-1^{-/-}* sesquimutants were significantly (~15%) lower than those in *nfu4-2* and *nfu5-1* single mutants (Figure 4a–d), suggesting that loss-of-function mutations in the *NFU4* and *NFU5* genes may have an additive effect. The amounts of chlorophyll *a*, chlorophyll *b*, carotenoid, and total chlorophyll in *nfu4-4^{-/-} nfu5-1^{+/-}* and *nfu4-4^{+/-} nfu5-1^{-/-}* sesquimutants showed similar trends (Figure 4a–d), especially when compared to the pigment levels in the *nfu5-1* single mutant.

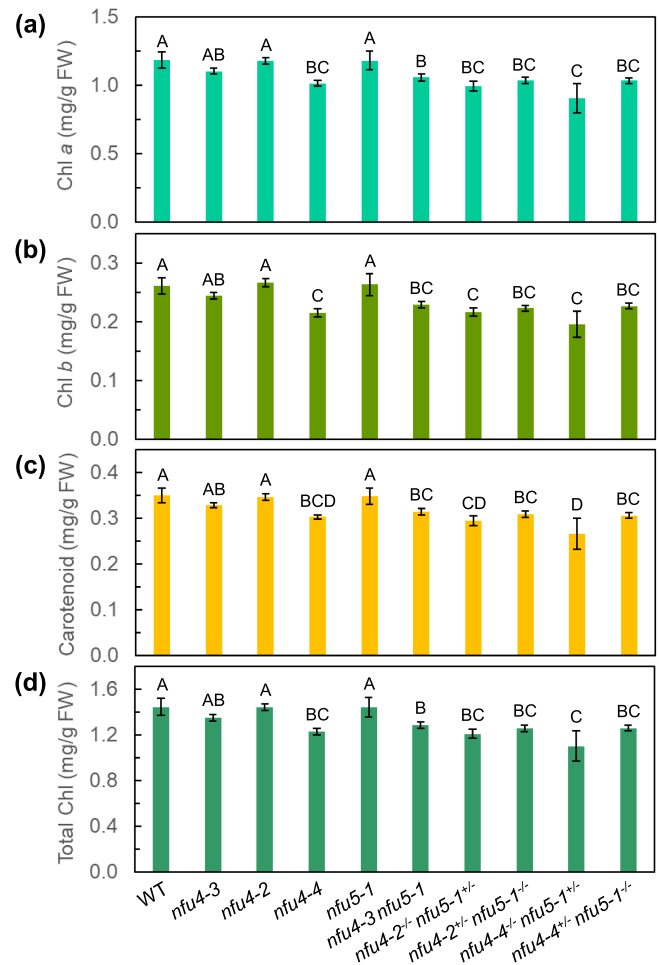


FIGURE 4 | Pigment contents in leaf tissues of 4-week-old plants. (a) Chlorophyll *a*, (b) chlorophyll *b*, (c) carotenoid, and (d) total chlorophyll contents in leaf tissues of 4-week-old plants. Values are presented as mean ± SE (*n* = 4 individual plants/genotype). Values not connected by the same uppercase letter are significantly different (Student's *t*-test, *p* < 0.05). FW, fresh weight; WT, wild type.

3.5 | The *NFU4* Transcript Was Abolished in *nfu4-2/4* Single Mutants and *nfu4-2/4^{-/-} nfu5-1^{+/-}* Sesquimutants

To investigate the functional relationship between *NFU4* and *NFU5* genes, we determined the relative levels of *NFU4* and *NFU5* transcripts in mature rosette leaves of 4-week-old plants with quantitative RT-PCR (Figure 5), using Power SYBR Green PCR master mix and qRT-PCR primers listed in Table S1. The housekeeping gene *ACTIN2* was used as an internal reference for transcript data normalization.

The *NFU4* transcript was not detected in *nfu4-2* and *nfu4-4* single mutants or *nfu4-2^{-/-} nfu5-1^{+/-}* and *nfu4-4^{-/-} nfu5-1^{+/-}* sesquimutants (Figure 5a). This observation is consistent with the previous report that the *NFU4* transcript was virtually absent in *nfu4-2* and *nfu4-4* (Przybyla-Toscano et al. 2022). *NFU4* transcripts levels in *nfu4-2^{+/-} nfu5-1^{-/-}* and *nfu4-4^{+/-} nfu5-1^{-/-}* sesquimutants were significantly (33% on average) lower than that in the Col wild type (Figure 5a), in line with the heterozygous *NFU4* genotype in these two sesquimutants.

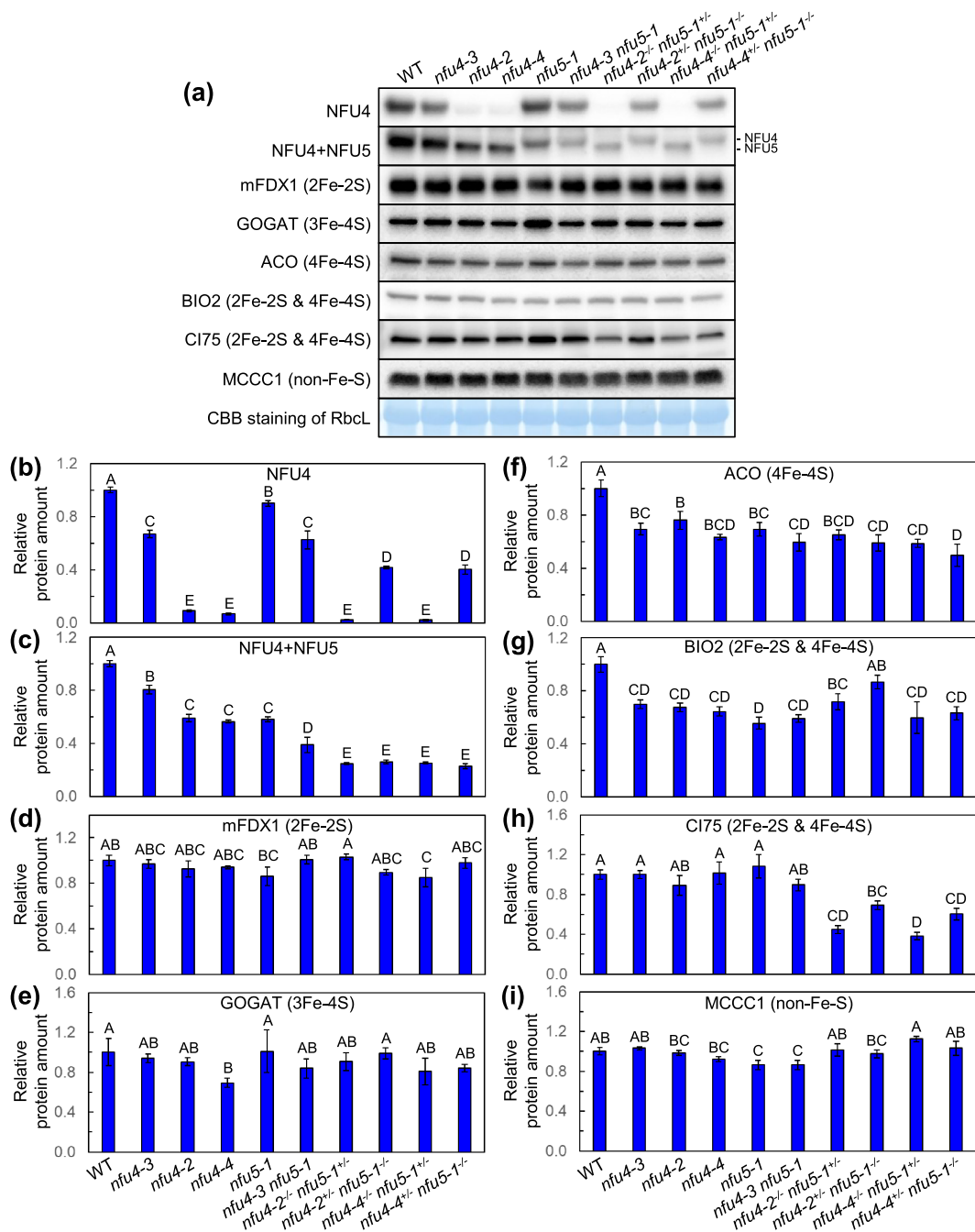


FIGURE 6 | Amounts of representative mitochondrial iron-sulfur proteins in leaf tissues of 4-week-old plants. (a) Representative immunoblots of mitochondrial iron-sulfur proteins in leaf tissues of 4-week-old plants. (b-i) Relative amounts of (b) NFU4, (c) NFU4 + NFU5, (d) 2Fe-2S protein mFDX1, (e) 3Fe-4S protein GOGAT, (f) 4Fe-4S protein ACO, (g) 2Fe-2S and 4Fe-4S proteins BIO2 and (h) CI75, and (i) non-Fe-S mitochondrial protein MCCC1 in leaf tissues of 4-week-old plants. In (b), blots were detected with the anti-NFU4 antibody. In (c), blots were detected with the anti-NFU4/NFU5 antibody, which cross-reacts with both NFU4 and NFU5. The mitochondrial protein MCCC1 does not contain any iron-sulfur (Fe-S) clusters and was used as a protein expected to be unaffected by changes in NFU4 and NFU5 abundances. Rubisco large subunit (Rbcl) stained with Coomassie Brilliant Blue was used as the loading control. Densitometric analysis of immunoblots was performed with the Multi Gauge V3.0 software; the average relative amount of each protein was normalized to 1.0 in the Col wild type (WT). Values are presented as mean \pm SE ($n = 3$ individual plants/genotype for NFU4 and NFU4 + NFU5 and $n = 4$ individual plants/genotype for other proteins). Values not connected by the same uppercase letter are significantly different (Student's *t*-test, $p < 0.05$).

nfu4-2/4^{+/-} nfu5-1^{-/-} sesquimutants were $\sim 75\%$ lower than that in the Col wild type and $\sim 57\%$ lower than those in *nfu4-2*, *nfu4-4*, and *nfu5-1* single mutants (Figure 6c). Similarly, the total level of NFU4 and NFU5 in the *nfu4-3* single mutant was 19% lower

than that in the Col wild type whereas the total level of NFU4 and NFU5 in the *nfu4-3 nfu5-1* double mutant was 61% lower than that in the Col wild type (Figure 6c). These observations demonstrated the additive effects of concurrent *nfu4* and *nfu5* mutations.

3.10 | Abundances of 2Fe–2S Protein mFDX1 and 3Fe–4S Protein GOGAT in Most *nfu4* and *nfu5-1* Single, Double, and Sesquimutants Were Not Significantly Different From Those in the Col Wild Type

To further investigate the roles of NFU4 and NFU5, we also determined the relative abundances of mitochondrion-targeted iron–sulfur proteins in mature rosette leaves of 4-week-old plants with SDS-PAGE and immunoblotting (Figure 6). We found that the levels of 2Fe–2S protein mFDX1 across the 10 genotypes were relatively uniform (Figure 6d). The only mutant with the mFDX1 protein level significantly lower than the Col wild type was *nfu4-4^{-/-} nfu5-1^{+/-}*, and the reduction was merely 15%. Although the level of 3Fe–4S protein GOGAT across the 10 genotypes (Figure 6e) was not as uniform as that of mFDX1, most mutants had a GOGAT protein level similar to the Col wild type. The only mutant with the GOGAT protein level significantly lower than the Col wild type was *nfu4-4*. These data are consistent with the hypothesis that loss-of-function mutations in the *NFU4* and *NFU5* genes do not appear to cause substantial changes in the abundances of mitochondrial 2Fe–2S proteins.

3.11 | Abundances of 4Fe–4S Protein ACO and 2Fe–2S and 4Fe–4S Protein BIO2 in Most *nfu4* and *nfu5-1* Single, Double, and Sesquimutants Were Significantly Lower Than Those in the Col Wild Type

We found that the contents of 4Fe–4S protein ACO in *nfu4* and *nfu5-1* single, double, and sesquimutants were significantly lower than that in the Col wild type (Figure 6f). The levels of ACO proteins in *nfu4* and *nfu5-1* single mutants were on average 31% lower than that in the Col wild type, and the levels of ACO proteins in the *nfu4-3 nfu5-1* double mutant and *nfu4-2/4^{-/-} nfu5-1^{+/-}* and *nfu4-2/4^{+/-} nfu5-1^{-/-}* sesquimutants were ~42% lower than that in the Col wild type on average. Similarly, the contents of 2Fe–2S and 4Fe–4S protein BIO2 in most *nfu4* and *nfu5-1* single, double, and sesquimutants were significantly (~34% on average) lower than that in the Col wild type (Figure 6g). These results are in line with the hypothesis that NFU4 and NFU5 may serve as iron–sulfur carriers during the biogenesis of mitochondrial 4Fe–4S clusters (Azam et al. 2020a) and that loss-of-function mutations in *NFU4* and *NFU5* genes negatively impact the levels of mitochondrial 4Fe–4S proteins.

3.12 | Levels of 2Fe–2S and 4Fe–4S Protein CI75 in *nfu4-2/4^{-/-} nfu5-1^{+/-}* and *nfu4-2/4^{+/-} nfu5-1^{-/-}* Sesquimutants Were Substantially Lower

We also discovered that the levels of 2Fe–2S and 4Fe–4S protein CI75 in *nfu4-2^{-/-} nfu5-1^{+/-}* and *nfu4-4^{-/-} nfu5-1^{+/-}* sesquimutants were on average 58% lower than those in the Col wild type and *nfu4-2*, *nfu4-4*, and *nfu5-1* single mutants (Figure 6h). Similarly, CI75 protein levels in *nfu4-2^{+/-} nfu5-1^{-/-}* and *nfu4-4^{+/-} nfu5-1^{-/-}* sesquimutants were on average 35% lower than those in the Col wild type, *nfu4-2*, *nfu4-4*, and *nfu5-1* (Figure 6h). These observations are consistent with the

hypothesis that NFU4 and NFU5 may serve as iron–sulfur carriers during the biogenesis of mitochondrial 4Fe–4S clusters (Azam et al. 2020a) and that loss-of-function mutations in *NFU4* and *NFU5* genes have an additive effect on the decreases of certain mitochondrial proteins containing 4Fe–4S. It is also worth mentioning that CI75 protein levels in *nfu4-2^{-/-} nfu5-1^{+/-}* and *nfu4-4^{-/-} nfu5-1^{+/-}* sesquimutants were ~36% lower than those in *nfu4-2^{+/-} nfu5-1^{-/-}* and *nfu4-4^{+/-} nfu5-1^{-/-}* sesquimutants. This observation suggests that NFU4 and NFU5 may have overlapping yet nonidentical functions.

The mitochondrial protein methylcrotononyl–CoA carboxylase 1 (MCCC1, i.e., the alpha subunit of the enzyme) does not contain any iron–sulfur clusters; therefore, we used this protein as a control. As expected, the levels of MCCC1 only varied slightly among the 10 genotypes (Figure 6i). Such minor differences in MCCC1 protein levels might be due to the semi-quantitative nature of immunoblotting.

3.13 | Correlation Analysis Among *NFU4/5* Transcripts, *NFU4/5* Proteins, Fresh Weights, Pigment Contents, and Mitochondrial Fe–S Proteins

To further investigate the functional relationships between NFU4 and NFU5, we performed correlation analysis among *NFU4/5* transcripts and *NFU4/5* proteins (Figure 7), using qRT-PCR, SDS-PAGE, and immunoblotting data of 4-week-old plants (Figures 5 and 6). The levels of both NFU4 and NFU5 proteins had a very strong positive correlation with the corresponding *NFU4* or *NFU5* transcript level (correlation coefficient $r=0.9055$ and 0.9699 , respectively; Figure 7a,b). This observation highlights the importance of *NFU4* and *NFU5* transcript levels to the abundances of NFU4 and NFU5 proteins. As expected, the total NFU4+NFU5 protein level had strong positive correlations with the level of individual NFU4 and NFU5 proteins (correlation coefficient $r=0.6082$ and 0.7048 , respectively; Figure 7c,d). This suggests that both NFU4 and NFU5 are important to the total NFU4+NFU5 protein level.

We also performed correlation analysis of fresh weights and pigment contents with NFU4/5 protein levels (Figure S1), using morphological, physiological, SDS-PAGE, and immunoblot data of 4-week-old plants (Figures 2, 4, and 6). The above-ground fresh weight had a very strong positive correlation ($r=0.8624$) with the NFU4 protein level, a very weak positive correlation ($r=0.1788$) with the NFU5 protein level, and a strong positive correlation ($r=0.7679$) with the total NFU4+NFU5 protein content (Figure S1a,d,g). The leaf carotenoid and total chlorophyll contents had strong positive correlations ($r=0.6833$ and 0.6660) with the NFU4 protein level, weak positive correlations ($r=0.2859$ and 0.2820) with the NFU5 protein level, and strong positive correlations ($r=0.7455$ and 0.7321) with the total NFU4+NFU5 protein content (Figure S1b–i). These observations suggest that NFU4 might be more important than NFU5 in influencing plant fresh weights and pigment contents.

Lastly, we performed correlation analysis between NFU4/5 protein levels and mitochondrial Fe–S protein contents (Figure 8),

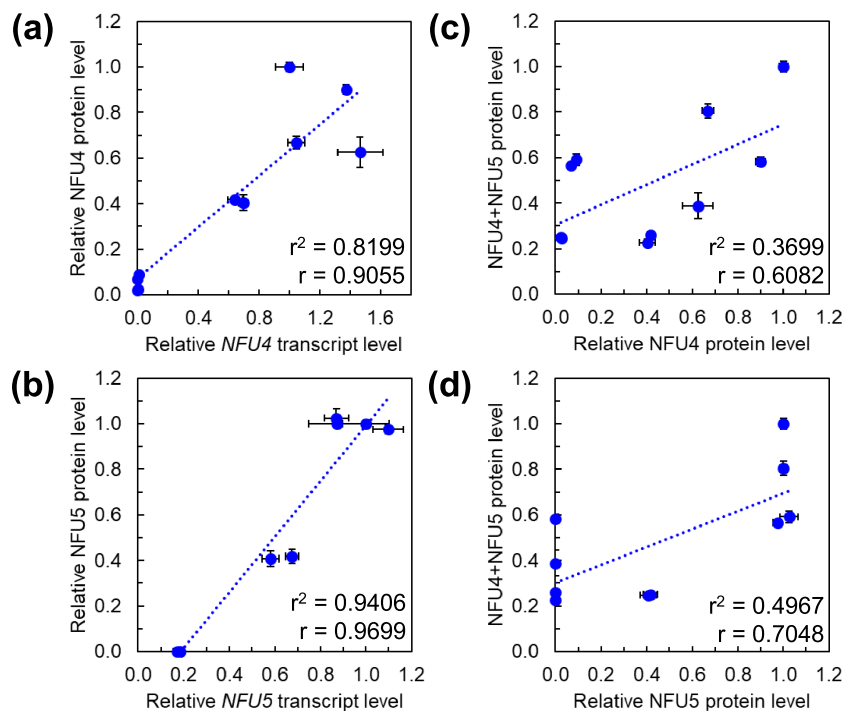


FIGURE 7 | Correlation analysis among the relative *NFU4* and *NFU5* transcript levels and the relative *NFU4* and *NFU5* protein levels in 4-week-old plants. (a) Correlation of the relative *NFU4* protein level on the relative *NFU4* transcript level; (b) correlation of the relative *NFU5* protein level on the relative *NFU5* transcript level; (c) correlation of the total amount of *NFU4* and *NFU5* proteins on the relative level of *NFU4* protein; and (d) correlation of the total amount of *NFU4* and *NFU5* proteins on the relative level of *NFU5* protein. Relative transcript levels were determined by qRT-PCR; the average ratio of *NFU4* or *NFU5* transcripts to *ACTIN2* transcripts was normalized to 1.0 in the Col WT, as shown in Figure 5. The relative *NFU4* protein level was determined by SDS-PAGE and immunoblotting with the anti-*NFU4* antibody; the total amount of *NFU4* and *NFU5* proteins was determined by SDS-PAGE and immunoblotting with the anti-*NFU5* antibody, which cross-reacts with *NFU4*; the relative *NFU5* protein level was calculated according to the relative levels of *NFU4* and *NFU4*+*NFU5* proteins; the average relative amount of each protein (*NFU4*, *NFU5*, and *NFU4*+*NFU4*) was normalized to 1.0 in the Col wild type (WT), as shown in Figure 6. Each blue point represents one genotype for the 10 genotypes shown in Figures 2 and 4–6. Error bars represent standard errors ($n=6$ individual plants/genotype for transcript levels and $n=3$ individual plants/genotype for protein levels). Dotted lines are linear regressions. The r -squared value and correlation coefficient r are also shown for each chart.

using SDS-PAGE and immunoblot data of 4-week-old plants (Figure 6). The level of 2Fe–2S protein mFDX1 had very weak positive correlations with *NFU4*, *NFU5*, and the total *NFU4*+*NFU5* protein level ($r=0.1097$, 0.1718 , and 0.1607 , respectively) (Figure 8a,g,m). This indicates that *NFU4/5* protein levels do not have a strong influence on the level of 2Fe–2S protein mFDX1. Interestingly, the level of 3Fe–4S protein GOGAT had a strong positive correlation ($r=0.6472$) with *NFU4*, a very weak negative correlation ($r=-0.1416$) with *NFU5*, and a weak positive correlation ($r=0.3360$) with the total *NFU4*+*NFU5* protein level (Figure 8b,h,n). It is unclear why the levels of 3Fe–4S protein GOGAT and *NFU4* had a strong positive correlation: As shown in Figure 6e, *nfu4-4* was the only mutant with the GOGAT protein level significantly lower than the Col wild type. The level of 4Fe–4S protein ACO had a moderate positive correlation ($r=0.4826$) with *NFU4*, a strong positive correlation ($r=0.6341$) with *NFU5*, and a very strong positive correlation ($r=0.8584$) with the total *NFU4*+*NFU5* protein level (Figure 8c,i,o). This suggests that both *NFU4* and *NFU5* are important to the level of 4Fe–4S protein ACO. The level of *BIO2*, which contains both 2Fe–2S and 4Fe–4S clusters, had weak positive correlations with individual *NFU4* and *NFU5* proteins ($r=0.3189$ and 0.3304 , respectively; Figure 8d,j). Consequently, *BIO2* had a moderate positive correlation with the total *NFU4*+*NFU5* protein level

($r=0.4383$; Figure 8p). The level of *CI75*, which contains both 2Fe–2S and 4Fe–4S clusters as well, had a strong positive correlation ($r=0.6291$) with *NFU4*, a weak positive correlation with *NFU5* ($r=0.3537$), and a strong positive correlation ($r=0.7788$) with the total *NFU4*+*NFU5* protein level (Figure 8e,k,q). This suggests that *NFU4* might be more important than *NFU5* in influencing the *CI75* protein level. To sum up, correlation analysis with SDS-PAGE and immunoblotting data revealed the relative importance of *NFU4* and *NFU5* proteins in influencing the levels of mitochondrial Fe–S proteins, especially 4Fe–4S protein ACO, and 2Fe–2S and 4Fe–4S proteins *BIO2* and *CI75*.

Taken together, spectroscopic and reconstitution analyses of recombinant *NFU4* and *NFU5* proteins plus morphological, physiological, and biochemical characterizations of *nfu4* and *nfu5-1* single, double, and sesquimutants collectively suggested that (1) *NFU4* and *NFU5* display UV-visible features characteristic of 4Fe–4S clusters and have an iron-sulfur scaffold function; (2) loss-of-function mutations in *NFU4* and *NFU5* genes negatively impact the levels of mitochondrial 4Fe–4S proteins, such as ACO, *BIO2*, and *CI75*; and (3) the simultaneous presence of loss-of-function mutations in *NFU4* and *NFU5* genes may have additive effects on plant growth and development, as well as 4Fe–4S biosynthesis in the mitochondrion.

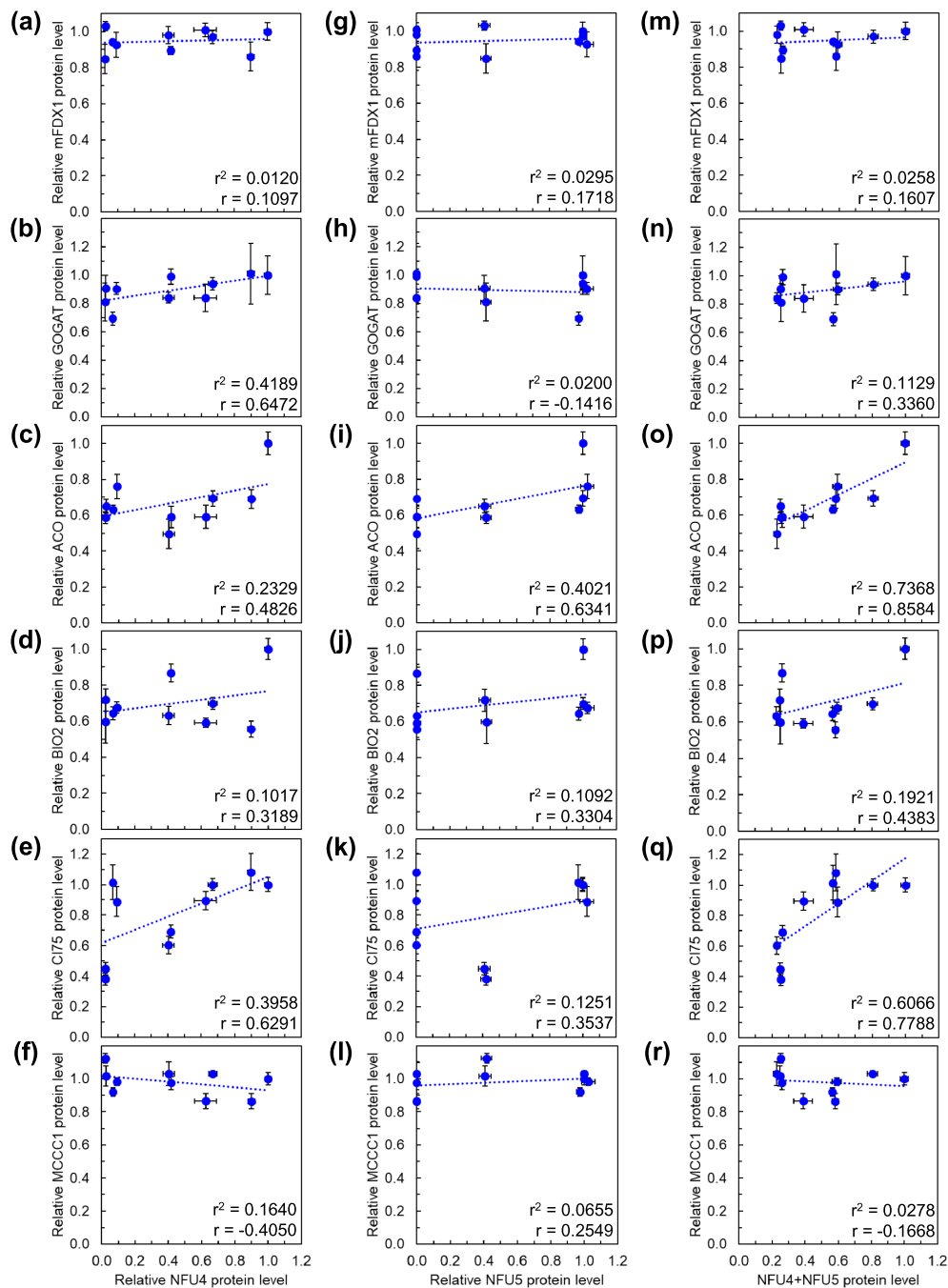


FIGURE 8 | Correlation analysis of the relative levels of mitochondrial iron-sulfur proteins with the relative NFU4 and NFU5 protein levels in 4-week-old plants. (a–f) Correlation analysis of the relative (a) mFDX1, (b) GOGAT, (c) ACO, (d) BIO2, (e) CI75, and (f) MCCC1 protein levels with the relative NFU4 protein level. (g–l) Correlation analysis of the relative (g) mFDX1, (h) GOGAT, (i) ACO, (j) BIO2, (k) CI75, and (l) MCCC1 protein levels with the relative NFU5 protein level. (m–r) Correlation analysis of the relative (m) mFDX1, (n) GOGAT, (o) ACO, (p) BIO2, (q) CI75, and (r) MCCC1 protein levels with the total NFU4 + NFU5 protein level. The relative NFU4 protein level was determined by SDS-PAGE and immunoblotting with the anti-NFU4 antibody; the total amount of NFU4 and NFU5 proteins was determined by SDS-PAGE and immunoblotting with the anti-NFU5 antibody, which cross-reacts with NFU4; the relative NFU5 protein level was calculated according to the relative levels of NFU4 and NFU4 + NFU5 proteins; the average relative amount of each protein (NFU4, NFU5, and NFU4 + NFU4) was normalized to 1.0 in the wild type (WT), as shown in Figure 6. Each blue point represents one genotype for the 10 genotypes shown in Figures 2 and 4–6. Error bars represent standard errors ($n = 3$ individual plants/genotype for NFU4, NFU5, and NFU4 + NFU5; $n = 4$ individual plants/genotype for other proteins). Dotted lines are linear regressions. The r -squared value and correlation coefficient r are also shown for each chart.

4 | Discussion

As mentioned previously, the two mitochondrion-targeted NFU proteins were previously proposed to participate in the biogenesis

of mitochondrial 4Fe–4S clusters (Azam et al. 2020a; Przybyla-Toscano et al. 2022). In this study, we showed that NFU4 and NFU5 proteins accommodate 4Fe–4S clusters and that loss-of-function mutations in the *NFU4* and *NFU5* genes resulted in

reduced levels of mitochondrial 4Fe–4S proteins. Consequently, *nfu4-2/4^{-/-} nfu5-1^{+/-}* and *nfu4-2/4^{+/-} nfu5-1^{-/-}* sesquimutants had a slightly smaller plant size than the Col wild type and the corresponding single mutants, and double homozygous, complete loss-of-function *nfu4 nfu5* mutants had an embryo-lethal phenotype. These observations demonstrate that NFU4 and NFU5 are essential in maintaining the levels of mitochondrial 4Fe–4S proteins. These results are also consistent with the hypothesis that NFU4 and NFU5 may serve as iron–sulfur carriers and may play a role in the transfer of 4Fe–4S clusters to recipient apoproteins during the biogenesis and maturation of mitochondrial 4Fe–4S clusters (Azam et al. 2020a).

4.1 | NFU4 and NFU5 Participate in the Biogenesis of 4Fe–4S Clusters in the Mitochondrion

The mitochondrial localization of NFU4 and NFU5 had been confirmed with green fluorescent protein tagging and confocal microscopy (Léon et al. 2003; Przybyla-Toscano et al. 2022). NFU proteins tend to exist as homodimers and two CXXC motifs (i.e., four cysteine residues) are required to coordinate one 4Fe–4S cluster (Roland et al. 2020; Przybyla-Toscano et al. 2022). Using spectroscopic analysis, we found that the affinity-purified recombinant NFU4 and NFU5 proteins each had a broad absorption peak at ~410 nm (Figure 1b,c), a characteristic feature of 4Fe–4S clusters (Kennedy et al. 1984; Nakamaru-Ogiso et al. 2002). This 410-nm absorption peak disappeared after the addition of the reducing agent sodium dithionite, suggesting that the 4Fe–4S cluster bound to NFU4 and NFU5 is redox labile (Nakamaru-Ogiso et al. 2002). In addition, *in vitro* reconstitution experiments (Figure 1b,c) showed that NFU4 and NFU5 have an iron–sulfur scaffold function. Furthermore, *nfu4-2/4^{-/-} nfu5-1^{+/-}* and *nfu4-2/4^{+/-} nfu5-1^{-/-}* sesquimutants showed reduced levels of 4Fe–4S protein ACO and reduced levels of 2Fe–2S and 4Fe–4S proteins BIO2 and CI75 (Figure 6f–h). These experiments are consistent with the hypothesis that NFU4 and NFU5 participate in the biogenesis of 4Fe–4S clusters in the mitochondrion.

4.2 | Simultaneous Presence of Loss-of-Function Mutations in NFU4 and NFU5 Genes Has Additive Effects on 4Fe–4S Biosynthesis and Mutant Phenotypes

As shown in Figure 6f,g, *nfu4* and *nfu5-1* single, double, and sesquimutants tended to have reduced levels of 4Fe–4S protein ACO and 2Fe–2S and 4Fe–4S protein BIO2. In addition, *nfu4-2/4^{-/-} nfu5-1^{+/-}* and *nfu4-2/4^{+/-} nfu5-1^{-/-}* sesquimutants had much lower levels of 2Fe–2S and 4Fe–4S protein CI75 than the Col wild type and the respective single mutants (Figure 6h). Consistent with the reduced levels of mitochondrial 4Fe–4S proteins, *nfu4^{-/-} nfu5-1^{+/-}* and *nfu4^{+/-} nfu5-1^{-/-}* sesquimutants appeared slightly smaller and had slightly lower amounts of carotenoid and chlorophyll than the Col wild type and the corresponding single mutants (Figures 2b,c and 4). Mitochondrial dysfunction has been found to affect chloroplast functions (Busi et al. 2011); therefore, it is not uncommon for mitochondrial iron–sulfur deficient mutants to have reduced amounts of carotenoid and chlorophyll. For example, knockdown mutants of the mitochondrial heat shock cognate B (HSCB) cochaperone

protein involved in iron–sulfur biosynthesis displayed 20%–40% reductions in chlorophyll content (Leaden et al. 2016). Furthermore, double homozygous, complete loss-of-function *nfu4-2/4 nfu5-1/3* mutants had an embryo-lethal phenotype (Figure 3). The slightly smaller phenotype of *nfu4-2/4 nfu5-1* sesquimutants and the embryo-lethal phenotype of double homozygous, complete loss-of-function *nfu4-2/4 nfu5-1* mutants had also been observed by Przybyla-Toscano et al. (2022). These data indicate that the simultaneous presence of loss-of-function mutations in *NFU4* and *NFU5* genes had additive effects on 4Fe–4S biosynthesis and mutant phenotypes.

4.3 | NFU4 and NFU5 May Play a Role in the Transfer of 4Fe–4S Clusters to Recipient Apoproteins in the Mitochondrion

As discussed previously, the abundances of 4Fe–4S protein ACO as well as 2Fe–2S and 4Fe–4S proteins BIO2 and CI75 were significantly reduced in *nfu4* and *nfu5-1* single mutants and/or sesquimutants (Figure 6f–h). Unlike these three proteins, the levels of 2Fe–2S protein mFDX1 and non-Fe–S protein MCCC1 across the 10 genotypes were relatively uniform (Figure 6d,i). These findings are consistent with the hypothesis that NFU4 and NFU5 may serve as iron–sulfur carriers during the biogenesis of mitochondrial 4Fe–4S clusters and may play a role in the transfer of 4Fe–4S clusters to recipient apoproteins (Azam et al. 2020a).

ACO is a key enzyme in the tricarboxylic acid cycle, which occurs in the mitochondrial matrix (Arnaud et al. 2007; Unciuleac et al. 2007; Hooks et al. 2014). An ACO monomer contains one 4Fe–4S cluster. In line with the proposed role of NFU4 and NFU5 in the maturation of ACO proteins, Navarro-Sastre et al. (2011) discovered that when yeast *Nfu1* gene (homologous to the *NFU4* and *NFU5* genes in *Arabidopsis*) was deleted, the yeast cells showed a 30% reduction in aconitase activity. Similarly, Przybyla-Toscano et al. (2022) found that *Arabidopsis* plants with absent *NFU4* expression and reduced *NFU5* expression (i.e., hemizygous *nfu4-2^{-/-} nfu5-1/nfu5-2* mutant plants) displayed a ~30% reduction in aconitase activity. However, Przybyla-Toscano et al. (2022) proposed that the effects of loss-of-function mutations in the *NFU4* and *NFU5* genes on aconitase activity might be due to carbon flux limitation, because the ACO protein level in the hemizygous *nfu4-2^{-/-} nfu5-1/nfu5-2* mutant did not appear to be significantly lower than that in the Col wild type, and the aconitase activity of the hemizygous *nfu4-2^{-/-} nfu5-1/nfu5-2* mutant recovered when grown under high CO₂ (i.e., 1%). Przybyla-Toscano et al. (2022) also found that ACO2 did not interact with NFU4 or NFU5 in yeast-two-hybrid assays. Despite these contradicting data in Przybyla-Toscano et al. (2022), we should still consider the potential role of NFU4 and NFU5 in ACO maturation for the following reasons. First, Przybyla-Toscano et al. (2022) did not report the aconitase activity of wild-type plants grown under high CO₂. Therefore, it is difficult to interpret the ACO activity increase in hemizygous *nfu4-2^{-/-} nfu5-1/nfu5-2* mutant plants grown under high CO₂. Second, Przybyla-Toscano et al. (2022) used total extracts from intact seedlings for aconitase activity assays but used mitochondrial extracts from callus for SDS-PAGE and immunoblotting.

Third, yeast-two-hybrid assays detect stable interactions, but the interactions between iron–sulfur carriers and recipient apoproteins are often transient (Braymer et al. 2021). Fourth, Azam et al. (2020a) actually found that the 4Fe–4S cluster bound to recombinant NFU4 and NFU5 proteins can be effectively transferred to recombinant apo-ACO2, one of the three ACO isoforms that is solely targeted to the mitochondrion. Although the in vitro activity of NFU4 and NFU5 proteins may differ from their in vivo activity, the biochemical data in Azam et al. (2020a) supported the proposed role of NFU4 and NFU5 in ACO maturation. Consistent with the proposed role of NFU4 and NFU5 in ACO maturation, our SDS-PAGE and immunoblot analysis showed that ACO protein levels in *nfu4* and *nfu5-1* single, double, and sesquimutants were significantly lower than that in the Col wild type (Figure 6f). In addition, the relative ACO protein level across the 10 genotypes used in this study correlated very strongly with the total NFU4 + NFU5 protein level ($r=0.8584$; Figure 8o). The discrepancy in ACO protein levels between this study and Przybyla-Toscano et al. (2022) might be because different tissues were used for protein extractions and subsequent SDS-PAGE and immunoblot analysis in these two studies: We used mature rosette leaves of 4-week-old plants; Przybyla-Toscano et al. (2022) used mitochondria isolated from callus.

BIO2 converts dethiobiotin to biotin in the mitochondrial matrix, and a BIO2 monomer contains one 2Fe–2S cluster and one 4Fe–4S cluster (Ugulava et al. 2001; Picciocchi et al. 2003). In the yeast mitochondrion, the 4Fe–4S cluster in the BIO2 protein was proposed to be delivered by Iba57 (57-kDa iron–sulfur cluster assembly factor for biotin synthase- and aconitase-like mitochondrial proteins), and the *Iba75*-deletion yeast strain displayed a ~40% reduction in biotin synthase activity (Gelling et al. 2008). In the higher plant *Arabidopsis*, most *nfu4* and *nfu5-1* single, double, and sesquimutants showed significant reductions (~34% on average) in BIO2 protein level (Figure 6g). This observation raised the possibility that the 4Fe–4S cluster in higher plant BIO2 protein can also be delivered by NFU4 and NFU5. It should be noted that BIO2 did not interact with NFU4 or NFU5 in the yeast-two-hybrid assays conducted by Przybyla-Toscano et al. (2022). However, we should not dismiss the potential role of NFU4 and NFU5 in BIO2 maturation. As mentioned previously, the interactions between iron–sulfur carriers and recipient apoproteins are most of the time transient or short lived (Braymer et al. 2021), and yeast-two-hybrid assays often detect stable interactions. Therefore, further biochemical studies are needed to explore the potential role of NFU4 and NFU5 in BIO2 maturation.

CI75 is the 75-kDa subunit of mitochondrial respiratory complex I, and this subunit contains one 2Fe–2S cluster and two 4Fe–4S clusters (Maldonado et al. 2020; López-López et al. 2022). Mitochondrial respiratory complex I contains >45 subunits, six 4Fe–4S clusters, and 2Fe–2S clusters in total (Maldonado et al. 2020; López-López et al. 2022). It was originally proposed that the 4Fe–4S clusters in complex I of higher plant mitochondrion are delivered by INDH (iron–sulfur protein required for NADH dehydrogenase) (Bych et al. 2008). Indeed, the *Arabidopsis indh* mutant exhibited a disrupted complex I and a near-complete absence of complex I activity (Wydro et al. 2013). However, Wydro et al. (2013) also found

that the amount of INDH protein did correlate well with the amount of fully assembled complex I. Further comparison of the *indh* mutant with mitochondrial translation mutants and complex I mutants indicated that INDH instead has a primary role in mitochondrial translation (Wydro et al. 2013). This finding triggered the search for other potential iron–sulfur carriers during the maturation of complex I proteins containing 4Fe–4S. In this work, the *Arabidopsis nfu4-2/4^{-/-} nfu5-1^{+/-}* and *nfu4-2/4^{+/-} nfu5-1^{-/-}* sesquimutants displayed substantial reductions in the level of CI75 (Figure 6h). Furthermore, the relative CI75 protein level across the 10 genotypes used in this study correlated strongly with the total NFU4 + NFU5 protein level ($r=0.7788$; Figure 8q). These observations suggest that NFU4 and NFU5 may serve as 4Fe–4S carriers during the maturation of CI75. It should be noted that Przybyla-Toscano et al. (2022) found that mitochondrial extracts from primary root cells of the hemizygous *nfu4-2^{-/-} nfu5-1/nfu5-2* mutant had similar complex I activity as those from primary root cells of the Col wild type. The discrepancy between CI75 protein levels in this study and complex I activities in Przybyla-Toscano et al. (2022) might be because different tissues were used in these two studies: We used mature rosette leaves of 4-week-old plants for protein extraction and subsequent SDS-PAGE and immunoblotting; Przybyla-Toscano et al. (2022) used mitochondria isolated from primary root cells for complex I activity assays. Therefore, we should not dismiss the potential role of NFU4 and NFU5 in CI75 maturation. Further biochemical studies are needed to explore this possibility.

NFU4 and NFU5 may play a role in the transfer of 4Fe–4S clusters to other apoproteins in the mitochondrion requiring 4Fe–4S. For example, NFU4 and NFU5 were found to interact with mitochondrial lipoyl synthase LIP1 in yeast-two-hybrid and bimolecular fluorescence complementation assays, and simultaneous loss-of-function mutations in the *NFU4* and *NFU5* genes resulted in substantial reductions in protein lipoylation (Przybyla-Toscano et al. 2022). Therefore, Przybyla-Toscano et al. (2022) proposed that NFU4 and NFU5 primarily serve as iron–sulfur carriers during the maturation of LIP1.

4.4 | Functional Relationship Between NFU4 and NFU5

As discussed previously, the biochemical characterization of recombinant NFU4 and NFU5 proteins (Figure 1b,c) and the embryo lethality of the double homozygous, complete loss-of-function *nfu4-2/4 nfu5-1/3* mutants (Figure 3) indicate that NFU4 and NFU5 are required in the biogenesis and maturation of mitochondrial 4Fe–4S clusters, consistent with the results in Przybyla-Toscano et al. (2022). Furthermore, the morphological, physiological, and biochemical characterizations of *nfu4* and *nfu5* single, double, and sesquimutants (Figures 2, 4, and 6) suggest that NFU4 and NFU5 have overlapping yet nonidentical functions.

During the correlation analysis, we found that NFU4 and NFU5 protein levels had very strong positive correlations with the respective *NFU4* and *NFU5* transcript levels (Figure 7a,b). This suggests that the regulation of NFU4 and NFU5 protein abundances primarily occurs at the transcriptional level. The

correlation studies also demonstrated that both NFU4 and NFU5 are important to the total NFU4 + NFU5 protein level (Figure 7c,d). According to Fuchs et al. (2020) and Przybyla-Toscano et al. (2022), the NFU4 protein was ~two-fold more abundant than the NFU5 protein in wild-type *Arabidopsis*. Therefore, loss-of-function mutations in the *NFU4* gene might be more impactful than the loss-of-function mutations in the *NFU5* gene. Consistent with this hypothesis, *nfu4-2/4^{-/-} nfu5-1^{+/-}* sesquimutants appeared slightly smaller than *nfu4-2/4^{+/-} nfu5-1^{-/-}* sesquimutants (Figure 2b,c). Interestingly, some of the mitochondrial 4Fe–4S proteins also followed this trend; for example, CI75 was significantly lower in *nfu4-2/4^{-/-} nfu5-1^{+/-}* than in *nfu4-2/4^{+/-} nfu5-1^{-/-}* (Figure 6h). Furthermore, the above-ground fresh weight across the 10 genotypes used in this study correlated better with the relative NFU4 protein level ($r=0.8624$; Figure S1a) than with the relative NFU5 protein level ($r=0.1788$; Figure S1d). Similarly, the relative CI75 protein level across the 10 genotypes used in this study correlated better with the relative NFU4 protein level ($r=0.6291$; Figure 8e) than with the relative NFU5 protein level ($r=0.3537$; Figure 8k). These observations suggest that NFU4 might be more important than NFU5 in influencing plant fresh weights and the levels of certain mitochondrial 4Fe–4S proteins (e.g., CI75).

5 | Conclusion

In conclusion, recombinant NFU4 and NFU5 proteins had an iron–sulfur scaffold function and displayed features characteristic of 4Fe–4S clusters. Immunoblot analysis of leaf extract showed that most *nfu4* and *nfu5-1* single, double, and sesquimutants had significant reductions in the levels of mitochondrial Fe–S proteins, such as 4Fe–4S protein aconitase (ACO) and 2Fe–2S and 4Fe–4S protein biotin synthase 2 (BIO2). In addition, the sesquimutants showed substantial reductions in the protein level of the 75-kDa subunit of respiratory complex I (CI75) containing 2Fe–2S and 4Fe–4S. These observations indicate that NFU4 and NFU5 are important, directly or indirectly, in maintaining the levels of mitochondrial 4Fe–4S proteins. Whether this is a consequence of the decreased activity of lipoate-dependent enzymes remains to be investigated.

Author Contributions

Yan Lu conceived and designed the project. Jun Zhao, Manasa B. Satyanarayan, Joshua T. VanSlambrouck, Alexander J. Kolstoe, Michael J. Voyt, Glory O. James, and Yan Lu performed the experiments and analyzed the data. Yan Lu wrote the manuscript. Fei Yu edited the manuscript.

Acknowledgments

The authors acknowledge Jessica Zhang (Portage Central High School), Audrey M. Searing (Western Michigan University [WMU]), Ruchi Ojha (WMU), and Jacob D. Waterlander (WMU) for technical assistance and Christopher D. Jackson (WMU) and Amanda Hyman (WMU) for growth chamber management. The authors are thankful to Dr. Nicolas Rouhier (Université de Lorraine) for donating the anti-NFU4 and anti-NFU4/5 antibodies. The authors are also thankful to Dr. Janneke Balk (John Innes Centre) for communications about the anti-NFU4 and anti-NFU4/5 antibodies.

Conflicts of Interest

The authors declare no conflicts of interest.

Data Availability Statement

All research data are included in the main text and supporting information. Sequence data of related genes/proteins can be found in the GenBank/EMBL databases under the following accession numbers: *NFU4*, At3g20970; *NFU5*, At1g51390; and *ACTIN2 (ACT2)*, At3g18780.

Peer Review

The peer review history for this article is available in the [Supporting Information](#) for this article.

References

- Alonso, J. M., A. N. Stepanova, T. J. Leisse, et al. 2003. "Genome-Wide Insertional Mutagenesis of *Arabidopsis thaliana*." *Science* 301, no. 5633: 653–657. <https://doi.org/10.1126/science.1086391>.
- Armas, A. M., M. Balparda, A. Terenzi, M. V. Busi, M. A. Pagani, and D. F. Gomez-Casati. 2020. "Iron–Sulfur Cluster Complex Assembly in the Mitochondria of *Arabidopsis thaliana*." *Plants* 9: 1171. <https://doi.org/10.3390/plants9091171>.
- Armas, A. M., M. Balparda, V. R. Turowski, M. V. Busi, M. A. Pagani, and D. F. Gomez-Casati. 2019. "Altered Levels of Mitochondrial NFS1 Affect Cellular Fe and S Contents in Plants." *Plant Cell Reports* 38: 981–990. <https://doi.org/10.1007/s00299-019-02419-9>.
- Arnaud, N., K. Ravet, A. Borlotti, et al. 2007. "The Iron-Responsive Element (IRE)/Iron-Regulatory Protein 1 (IRP1)-Cytosolic Aconitase Iron-Regulatory Switch Does Not Operate in Plants." *Biochemical Journal* 405: 523–531. <https://doi.org/10.1042/bj20061874>.
- Azam, T., J. Przybyla-Toscano, F. Vignols, J. Couturier, N. Rouhier, and M. K. Johnson. 2020a. "[4Fe–4S] Cluster Trafficking Mediated by *Arabidopsis* Mitochondrial ISCA and NFU Proteins." *Journal of Biological Chemistry* 295: 18367–18378. <https://doi.org/10.1074/jbc.RA120.015726>.
- Azam, T., J. Przybyla-Toscano, F. Vignols, J. Couturier, N. Rouhier, and M. K. Johnson. 2020b. "The *Arabidopsis* Mitochondrial Glutaredoxin GRXS15 Provides [2Fe–2S] Clusters for ISCA-Mediated [4Fe–4S] Cluster Maturation." *International Journal of Molecular Sciences* 21: 9237. <https://doi.org/10.3390/ijms21239237>.
- Balk, J., and S. Lobréaux. 2005. "Biogenesis of Iron–Sulfur Proteins in Plants." *Trends in Plant Science* 10: 324–331. <https://doi.org/10.1016/j.tplants.2005.05.002>.
- Balk, J., and M. Pilon. 2011. "Ancient and Essential: The Assembly of Iron–Sulfur Clusters in Plants." *Trends in Plant Science* 16: 218–226. <https://doi.org/10.1016/j.tplants.2010.12.006>.
- Balk, J., and T. A. Schaedler. 2014. "Iron Cofactor Assembly in Plants." *Annual Review of Plant Biology* 65: 125–153. <https://doi.org/10.1146/annurev-arplant-050213-035759>.
- Bandyopadhyay, S., F. Gama, M. M. Molina-Navarro, et al. 2008. "Chloroplast Monothiol Glutaredoxins as Scaffold Proteins for the Assembly and Delivery of [2Fe–2S] Clusters." *EMBO Journal* 27: 1122–1133. <https://doi.org/10.1038/emboj.2008.50>.
- Beinert, H. 2000. "Iron–Sulfur Proteins: Ancient Structures, Still Full of Surprises." *Journal of Biological Inorganic Chemistry* 5: 2–15. <https://doi.org/10.1007/s007750050002>.
- Berger, N., F. Vignols, J. Przybyla-Toscano, et al. 2020b. "Identification of Client Iron–Sulfur Proteins of the Chloroplastic NFU2 Transfer Protein in *Arabidopsis thaliana*." *Journal of Experimental Botany* 71: 4171–4187. <https://doi.org/10.1093/jxb/eraa166>.

- Berger, N., F. Vignols, B. Touraine, et al. 2020a. "A Global Proteomic Approach Sheds New Light on Potential Iron–Sulfur Client Proteins of the Chloroplastic Maturation Factor NFU3." *International Journal of Molecular Sciences* 21: 8121. <https://doi.org/10.3390/ijms21218121>.
- Berndt, C., L. Christ, N. Rouhier, and U. Mühlenhoff. 2021. "Glutaredoxins With Iron–Sulphur Clusters in Eukaryotes – Structure, Function and Impact on Disease." *Biochimica et Biophysica Acta – Bioenergetics* 1862: 148317. <https://doi.org/10.1016/j.bbabi.2020.148317>.
- Braymer, J. J., S. A. Freibert, M. Rakwalska-Bange, and R. Lill. 2021. "Mechanistic Concepts of Iron–Sulfur Protein Biogenesis in Biology." *Biochimica et Biophysica Acta, Molecular Cell Research* 1868: 118863. <https://doi.org/10.1016/j.bbamcr.2020.118863>.
- Braymer, J. J., and R. Lill. 2017. "Iron–Sulfur Cluster Biogenesis and Trafficking in Mitochondria." *Journal of Biological Chemistry* 292: 12754–12763. <https://doi.org/10.1074/jbc.R117.787101>.
- Busi, M. V., M. E. Gomez-Lobato, A. Araya, and D. F. Gomez-Casati. 2011. "Mitochondrial Dysfunction Affects Chloroplast Functions." *Plant Signaling and Behavior* 6: 1904–1907. <https://doi.org/10.4161/psb.6.12.18050>.
- Busi, M. V., M. V. Maliandi, H. Valdez, et al. 2006. "Deficiency of *Arabidopsis thaliana* Frataxin Alters Activity of Mitochondrial Fe–S Proteins and Induces Oxidative Stress." *Plant Journal* 48: 873–882. <https://doi.org/10.1111/j.1365-313X.2006.02923.x>.
- Bych, K., D. J. A. Netz, G. Vigani, et al. 2008. "The Essential Cytosolic Iron–Sulfur Protein Nbp35 Acts Without Cfd1 Partner in the Green Lineage." *Journal of Biological Chemistry* 283: 35797–35804. <https://doi.org/10.1074/jbc.M807303200>.
- Caubrière, D., A. Moseler, N. Rouhier, and J. Couturier. 2023. "Diversity and Roles of Cysteine Desulfurases in Photosynthetic Organisms." *Journal of Experimental Botany* 74: 3345–3360. <https://doi.org/10.1093/jxb/erad065>.
- Clark, T. J., and Y. Lu. 2015. "Analysis of Loss-Of-Function Mutants in Aspartate Kinase and Homoserine Dehydrogenase Genes Points to Complexity in the Regulation of Aspartate-Derived Amino Acid Contents." *Plant Physiology* 168: 1512–1526. <https://doi.org/10.1104/pp.15.00364>.
- Couturier, J., J. Przybyla-Toscano, T. Roret, C. Didierjean, and N. Rouhier. 2015. "The Roles of Glutaredoxins Ligating Fe–S Clusters: Sensing, Transfer or Repair Functions?" *Biochimica et Biophysica Acta, Molecular Cell Research* 1853: 1513–1527. <https://doi.org/10.1016/j.bbamcr.2014.09.018>.
- Couturier, J., B. Touraine, J. F. Briat, F. Gaymard, and N. Rouhier. 2013. "The Iron–Sulfur Cluster Assembly Machineries in Plants: Current Knowledge and Open Questions." *Frontiers in Plant Science* 4: 259. <https://doi.org/10.3389/fpls.2013.00259>.
- Couturier, J., H. C. Wu, T. Dhalleine, et al. 2014. "Monothiol Glutaredoxin–BolA Interactions: Redox Control of *Arabidopsis thaliana* BolA2 and SufE1." *Molecular Plant* 7: 187–205. <https://doi.org/10.1093/mp/sst156>.
- de Ollas, C., C. Segarra-Medina, M. González-Guzmán, J. Puertolas, and A. Gómez-Cadenas. 2019. "A Customizable Method to Characterize *Arabidopsis thaliana* Transpiration Under Drought Conditions." *Plant Methods* 15: 89. <https://doi.org/10.1186/s13007-019-0474-0>.
- Fonseca, J. P., H. K. Lee, C. Boschiero, et al. 2020. "Iron–Sulfur Cluster Protein NITROGEN FIXATION S-LIKE1 and Its Interactor FRATAXIN Function in Plant Immunity." *Plant Physiology* 184: 1532–1548. <https://doi.org/10.1104/pp.20.00950>.
- Frazzon, A. P., M. V. Ramirez, U. Warek, et al. 2007. "Functional Analysis of *Arabidopsis* Genes Involved in Mitochondrial Iron–Sulfur Cluster Assembly." *Plant Molecular Biology* 64: 225–240. <https://doi.org/10.1007/s11103-007-9147-x>.
- Fu, X., X. Guan, R. Garlock, and B. J. Nikolau. 2020. "Mitochondrial Fatty Acid Synthase Utilizes Multiple Acyl Carrier Protein Isoforms." *Plant Physiology* 183: 547–557. <https://doi.org/10.1104/pp.19.01468>.
- Fuchs, P., N. Rugen, C. Carrie, et al. 2020. "Single Organelle Function and Organization as Estimated From *Arabidopsis* Mitochondrial Proteomics." *Plant Journal* 101: 420–441. <https://doi.org/10.1111/tbj.14534>.
- Gelling, C., I. W. Dawes, N. Richhardt, R. Lill, and U. Mühlenhoff. 2008. "Mitochondrial Iba57p Is Required for Fe/S Cluster Formation on Aconitase and Activation of Radical SAM Enzymes." *Molecular and Cellular Biology* 28: 1851–1861. <https://doi.org/10.1128/mcb.01963-07>.
- Hackett, J. B., X. Shi, A. T. Kobylarz, et al. 2017. "An Organelle RNA Recognition Motif Protein Is Required for Photosystem II Subunit *psbF* Transcript Editing." *Plant Physiology* 173: 2278–2293. <https://doi.org/10.1104/pp.16.01623>.
- Hooks, M. A., J. W. Allwood, J. K. D. Harrison, et al. 2014. "Selective Induction and Subcellular Distribution of Aconitase 3 Reveal the Importance of Cytosolic Citrate Metabolism During Lipid Mobilization in *Arabidopsis*." *Biochemical Journal* 463: 309–317. <https://doi.org/10.1042/BJ20140430>.
- Ivanova, A., M. Gill-Hille, S. Huang, et al. 2019. "A Mitochondrial LYR Protein Is Required for Complex I Assembly." *Plant Physiology* 181: 1632–1650. <https://doi.org/10.1104/pp.19.00822>.
- Johnson, D. C., D. R. Dean, A. D. Smith, and M. K. Johnson. 2005. "Structure, Function, and Formation of Biological Iron–Sulfur Clusters." *Annual Review of Biochemistry* 74: 247–281. <https://doi.org/10.1146/annurev.biochem.74.082803.133518>.
- Kairis, A., B. D. Neves, J. Couturier, C. Remacle, and N. Rouhier. 2024. "Iron–Sulfur Cluster Synthesis in Plastids by the SUF System: A Mechanistic and Structural Perspective." *Biochimica et Biophysica Acta, Molecular Cell Research* 1871: 119797. <https://doi.org/10.1016/j.bbamcr.2024.119797>.
- Kennedy, M. C., T. A. Kent, M. Emptage, H. Merkle, H. Beinert, and E. Munck. 1984. "Evidence for the Formation of a Linear [3Fe–4S] Cluster in Partially Unfolded Aconitase." *Journal of Biological Chemistry* 259: 14463–14471. <https://pubmed.ncbi.nlm.nih.gov/6094558/>.
- Leaden, L., M. V. Busi, and D. F. Gomez-Casati. 2014. "The Mitochondrial Proteins AtHscB and AtIsu1 Involved in Fe–S Cluster Assembly Interact With the Hsp70-Type Chaperon AtHscA2 and Modulate Its Catalytic Activity." *Mitochondrion* 19: 375–381. <https://doi.org/10.1016/j.mito.2014.11.002>.
- Leaden, L., M. A. Pagani, M. Balparda, M. V. Busi, and D. F. Gomez-Casati. 2016. "Altered Levels of AtHSCB Disrupts Iron Translocation From Roots to Shoots." *Plant Molecular Biology* 92: 613–628. <https://doi.org/10.1007/s11103-016-0537-9>.
- Léon, S., B. Touraine, J. F. Briat, and S. Lobléaux. 2002. "The *AtNFS2* Gene From *Arabidopsis thaliana* Encodes a NifS-Like Plastidial Cysteine Desulphurase." *Biochemical Journal* 366: 557–564. <https://doi.org/10.1042/bj20020322>.
- Léon, S., B. Touraine, J.-F. Briat, and S. Lobléaux. 2005. "Mitochondrial Localization of *Arabidopsis thaliana* Isu Fe–S Scaffold Proteins." *FEBS Letters* 579: 1930–1934. <https://doi.org/10.1016/j.febslet.2005.02.038>.
- Léon, S., B. Touraine, C. Ribot, J. F. Briat, and S. Lobléaux. 2003. "Iron–Sulphur Cluster Assembly in Plants: Distinct NFU Proteins in Mitochondria and Plastids From *Arabidopsis thaliana*." *Biochemical Journal* 371: 823–830. <https://doi.org/10.1042/BJ20021946>.
- Li, Y., K. Belt, S. F. Alqahtani, et al. 2022. "The Mitochondrial LYR Protein SDHAF1 Is Required for Succinate Dehydrogenase Activity in *Arabidopsis*." *Plant Journal* 110: 499–512. <https://doi.org/10.1111/tbj.15684>.
- Lill, R. 2009. "Function and Biogenesis of Iron–Sulphur Proteins." *Nature* 460: 831–838. <https://doi.org/10.1038/nature08301>.

- Lill, R., and G. Kispal. 2000. "Maturation of Cellular Fe-S Proteins: An Essential Function of Mitochondria." *Trends in Biochemical Sciences* 25: 352–356. [https://doi.org/10.1016/s0968-0004\(00\)01589-9](https://doi.org/10.1016/s0968-0004(00)01589-9).
- Lill, R., and U. Muhlenhoff. 2008. "Maturation of Iron-Sulfur Proteins in Eukaryotes: Mechanisms, Connected Processes, and Diseases." *Annual Review of Biochemistry* 77: 669–700. <https://doi.org/10.1146/annurev.biochem.76.052705.162653>.
- López-López, A., O. Keech, and N. Rouhier. 2022. "Maturation and Assembly of Iron-Sulfur Cluster-Containing Subunits in the Mitochondrial Complex I From Plants." *Frontiers in Plant Science* 13: 916948. <https://doi.org/10.3389/fpls.2022.916948>.
- Lu, Y. 2018. "Assembly and Transfer of Iron-Sulfur Clusters in the Plastid." *Frontiers in Plant Science* 9: 336. <https://doi.org/10.3389/fpls.2018.00336>.
- Maldonado, M., A. Padavannil, L. Zhou, F. Guo, and J. A. Letts. 2020. "Atomic Structure of a Mitochondrial Complex I Intermediate From Vascular Plants." *eLife* 9: e56664. <https://doi.org/10.7554/eLife.56664>.
- Meghanathan, N. 2016. "Assortativity Analysis of Real-World Network Graphs Based on Centrality Metrics." *Computer and Information Science* 9: 7–25. <https://doi.org/10.5539/cis.v9n3p7>.
- Moseler, A., I. Aller, S. Wagner, et al. 2015. "The Mitochondrial Monothiol Glutaredoxin S15 Is Essential for Iron-Sulfur Protein Maturation in *Arabidopsis thaliana*." *Proceedings of the National Academy of Sciences of the United States of America* 112: 13735–13740. <https://doi.org/10.1073/pnas.1510835112>.
- Moseler, A., I. Kruse, A. E. Maclean, et al. 2021. "The Function of Glutaredoxin GRXS15 Is Required for Lipoyl-Dependent Dehydrogenases in Mitochondria." *Plant Physiology* 186: 1507–1525. <https://doi.org/10.1093/plphys/kiab172>.
- Nakamaru-Ogiso, E., T. Yano, T. Ohnishi, and T. Yagi. 2002. "Characterization of the Iron-Sulfur Cluster Coordinated by a Cysteine Cluster Motif (CXXCXXXCX₂₇C) in the Nqo3 Subunit in the Proton-Translocating NADH-Quinone Oxidoreductase (NDH-1) of *Thermus thermophilus* HB-8." *Journal of Biological Chemistry* 277: 1680–1688. <https://doi.org/10.1074/jbc.M108796200>.
- Nath, K., J. P. O'Donnell, and Y. Lu. 2017. "Chloroplastic Iron-Sulfur Scaffold Protein NFU3 Is Essential to Overall Plant Fitness." *Plant Signaling and Behavior* 12: e1282023. <https://doi.org/10.1080/15592324.2017.1282023>.
- Nath, K., R. L. Wessendorf, and Y. Lu. 2016. "A Nitrogen-Fixing Subunit Essential for Accumulating 4Fe-4S-Containing Photosystem I Core Proteins." *Plant Physiology* 172: 2459–2470. <https://doi.org/10.1104/pp.16.01564>.
- Navarro-Sastre, A., F. Tort, O. Stehling, et al. 2011. "A Fatal Mitochondrial Disease Is Associated With Defective NFU1 Function in the Maturation of a Subset of Mitochondrial Fe-S Proteins." *American Journal of Human Genetics* 89: 656–667. <https://doi.org/10.1016/j.ajhg.2011.10.005>.
- Pan, X., H. Liu, J. Clarke, J. Jones, M. Bevan, and L. Stein. 2003. "ATIDB: *Arabidopsis thaliana* Insertion Database." *Nucleic Acids Research* 31: 1245–1251. <https://doi.org/10.1093/nar/gkg222>.
- Pedroletti, L., A. Moseler, and A. J. Meyer. 2023. "Assembly, Transfer, and Fate of Mitochondrial Iron-Sulfur Clusters." *Journal of Experimental Botany* 74: 3328–3344. <https://doi.org/10.1093/jxb/erad062>.
- Picciochi, A., R. Douce, and C. Alban. 2003. "The Plant Biotin Synthase Reaction. Identification and Characterization of Essential Mitochondrial Accessory Protein Components." *Journal of Biological Chemistry* 278: 24966–24975. <https://doi.org/10.1074/jbc.M302154200>.
- Pilon, M., S. E. Abdel-Ghany, D. Van Hoewyk, H. Ye, and E. A. Pilon-Smits. 2006. "Biogenesis of Iron-Sulfur Cluster Proteins in Plastids." *Genetic Engineering* 27: 101–117. https://doi.org/10.1007/0-387-25856-6_7.
- Przybyla-Toscano, J., C. Boussardon, S. R. Law, N. Rouhier, and O. Keech. 2021a. "Gene Atlas of Iron-Containing Proteins in *Arabidopsis thaliana*." *Plant Journal* 106: 258–274. <https://doi.org/10.1111/tpj.15154>.
- Przybyla-Toscano, J., L. Christ, O. Keech, and N. Rouhier. 2021b. "Iron-Sulfur Proteins in Plant Mitochondria: Roles and Maturation." *Journal of Experimental Botany* 72: 2014–2044. <https://doi.org/10.1093/jxb/eraa578>.
- Przybyla-Toscano, J., J. Couturier, C. Remacle, and N. Rouhier. 2021c. "Occurrence, Evolution and Specificities of Iron-Sulfur Proteins and Maturation Factors in Chloroplasts From Algae." *International Journal of Molecular Sciences* 22: 3175. <https://doi.org/10.3390/ijms22063175>.
- Przybyla-Toscano, J., A. E. Maclean, M. Franceschetti, et al. 2022. "Protein Lipoylation in Mitochondria Requires Fe-S Cluster Assembly Factors NFU4 and NFU5." *Plant Physiology* 188: 997–1013. <https://doi.org/10.1093/plphys/kiab501>.
- Przybyla-Toscano, J., M. Roland, F. Gaymard, J. Couturier, and N. Rouhier. 2018. "Roles and Maturation of Iron-Sulfur Proteins in Plastids." *Journal of Biological Inorganic Chemistry* 23: 545–566. <https://doi.org/10.1007/s00775-018-1532-1>.
- Roland, M., J. Przybyla-Toscano, F. Vignols, et al. 2020. "The Plastidial *Arabidopsis thaliana* NFU1 Protein Binds and Delivers [4Fe-4S] Clusters to Specific Client Proteins." *Journal of Biological Chemistry* 295: 1727–1742. <https://doi.org/10.1074/jbc.RA119.011034>.
- Rouhier, N., J. Couturier, M. K. Johnson, and J.-P. Jacquot. 2010. "Glutaredoxins: Roles in Iron Homeostasis." *Trends in Biochemical Sciences* 35: 43–52. <https://doi.org/10.1016/j.tibs.2009.08.005>.
- Satyanarayan, M. B., J. Zhao, J. Zhang, F. Yu, and Y. Lu. 2021. "Functional Relationships of Three NFU Proteins in the Biogenesis of Chloroplastic Iron-Sulfur Clusters." *Plant Direct* 5: e00303. <https://doi.org/10.1002/pld3.303>.
- Schwenkert, S., D. J. Netz, J. Frazzon, et al. 2010. "Chloroplast HCF101 Is a Scaffold Protein for [4Fe-4S] Cluster Assembly." *Biochemical Journal* 425: 207–214. <https://doi.org/10.1042/BJ20091290>.
- Talib, E. A., and C. E. Outten. 2021. "Iron-Sulfur Cluster Biogenesis, Trafficking, and Signaling: Roles for CGFS Glutaredoxins and BolA Proteins." *Biochimica et Biophysica Acta, Molecular Cell Research* 1868: 118847. <https://doi.org/10.1016/j.bbamcr.2020.118847>.
- Touraine, B., J. P. Boutin, A. Marion-Poll, J. F. Briat, G. Peltier, and S. Lobréaux. 2004. "Nfu2: A Scaffold Protein Required for [4Fe-4S] and Ferredoxin Iron-Sulphur Cluster Assembly in *Arabidopsis* Chloroplasts." *Plant Journal* 40: 101–111. <https://doi.org/10.1111/j.1365-313X.2004.02189.x>.
- Touraine, B., F. Vignols, J. Przybyla-Toscano, et al. 2019. "Iron-Sulfur Protein NFU2 Is Required for Branched-Chain Amino Acid Synthesis in *Arabidopsis* Roots." *Journal of Experimental Botany* 70: 1875–1889. <https://doi.org/10.1093/jxb/erz050>.
- Turowski, V. R., M. V. Busi, and D. F. Gomez-Casati. 2012. "Structural and Functional Studies of the Mitochondrial Cysteine Desulfurase From *Arabidopsis thaliana*." *Molecular Plant* 5: 1001–1010. <https://doi.org/10.1093/mp/sss037>.
- Ugulava, N. B., B. R. Gibney, and J. T. Jarrett. 2001. "Biotin Synthase Contains Two Distinct Iron-Sulfur Cluster Binding Sites: Chemical and Spectroelectrochemical Analysis of Iron-Sulfur Cluster Interconversions." *Biochemistry* 40: 8343–8351. <https://doi.org/10.1021/bi0104625>.
- Unciuleac, M.-C., K. Chandramouli, S. Naik, et al. 2007. "In Vitro Activation of Apo-Aconitase Using a [4Fe-4S] Cluster-Loaded Form of

the IscU [Fe–S] Cluster Scaffolding Protein.” *Biochemistry* 46: 6812–6821. <https://doi.org/10.1021/bi6026665>.

Uzarska, M. A., J. Przybyla-Toscano, F. Spantgar, et al. 2018. “Conserved Functions of *Arabidopsis* Mitochondrial Late-Acting Maturation Factors in the Trafficking of Iron–Sulfur Clusters.” *Biochimica et Biophysica Acta, Molecular Cell Research* 1865: 1250–1259. <https://doi.org/10.1016/j.bbamcr.2018.06.003>.

Vazzola, V., A. Losa, C. Soave, and I. Murgia. 2007. “Knockout of Frataxin Gene Causes Embryo Lethality in *Arabidopsis*.” *FEBS Letters* 581: 667–672. <https://doi.org/10.1016/j.febslet.2007.01.030>.

Waller, J. C., S. Alvarez, V. Naponelli, et al. 2010. “A Role for Tetrahydrofolates in the Metabolism of Iron–Sulfur Clusters in All Domains of Life.” *Proceedings of the National Academy of Sciences of the United States of America* 107: 10412–10417. <https://doi.org/10.1073/pnas.0911586107>.

Waller, J. C., K. W. Ellens, S. Alvarez, K. Loizeau, S. Ravel, and A. D. Hanson. 2012. “Mitochondrial and Plastidial COG0354 Proteins Have Folate-Dependent Functions in Iron–Sulphur Cluster Metabolism.” *Journal of Experimental Botany* 63: 403–411. <https://doi.org/10.1093/jxb/err286>.

Wang, P. 2022. “Last Piece of the Puzzle: Defining Client Proteins of the NFU Iron–Sulfur Transfer Proteins in Mitochondria.” *Plant Physiology* 188: 928–930. <https://doi.org/10.1093/plphys/kiab523>.

Weiler, B. D., M.-C. Brück, I. Kothe, E. Bill, R. Lill, and U. Mühlenhoff. 2020. “Mitochondrial [4Fe–4S] Protein Assembly Involves Reductive [2Fe–2S] Cluster Fusion on ISCA1–ISCA2 by Electron Flow From Ferredoxin FDX2.” *Proceedings of the National Academy of Sciences of the United States of America* 117: 20555–20565. <https://doi.org/10.1073/pnas.2003982117>.

Wellburn, A. R. 1994. “The Spectral Determination of Chlorophyll *a* and Chlorophyll *b*, as Well as Total Carotenoids, Using Various Solvents with Spectrophotometers of Different Resolution.” *Journal of Plant Physiology* 144: 307–313. [https://doi.org/10.1016/S0176-1617\(11\)81192-2](https://doi.org/10.1016/S0176-1617(11)81192-2).

Woody, S. T., S. Austin-Phillips, R. M. Amasino, and P. J. Krysan. 2007. “The WiscDsLox T-DNA Collection: An *Arabidopsis* Community Resource Generated by Using an Improved High-Throughput T-DNA Sequencing Pipeline.” *Journal of Plant Research* 120: 157–165. <https://doi.org/10.1007/s10265-006-0048-x>.

Wydro, M. M., P. Sharma, J. M. Foster, K. Bych, E. H. Meyer, and J. Balk. 2013. “The Evolutionarily Conserved Iron–Sulfur Protein INDH Is Required for Complex I Assembly and Mitochondrial Translation in *Arabidopsis*.” *Plant Cell* 25: 4014–4027. <https://doi.org/10.1105/tpc.113.117283>.

Xu, X. M., H. Lin, M. Latijnhouwers, and S. G. Møller. 2009. “Dual Localized AtHscB Involved in Iron–Sulfur Protein Biogenesis in *Arabidopsis*.” *PLoS ONE* 4: e7662. <https://doi.org/10.1371/journal.pone.0007662>.

Xu, X. M., and S. G. Møller. 2006. “AtSufE Is an Essential Activator of Plastidic and Mitochondrial Desulfurases in *Arabidopsis*.” *EMBO Journal* 25: 900–909. <https://doi.org/10.1038/sj.emboj.7600968>.

Yabe, T., K. Morimoto, S. Kikuchi, K. Nishio, I. Terashima, and M. Nakai. 2004. “The *Arabidopsis* Chloroplastic NifU-Like Protein CnfU, Which Can Act As an Iron–Sulfur Cluster Scaffold Protein, Is Required for Biogenesis of Ferredoxin and Photosystem I.” *Plant Cell* 16: 993–1007. <https://doi.org/10.1105/tpc.020511>.

Yabe, T., and M. Nakai. 2006. “*Arabidopsis* AtIscA-I Is Affected by Deficiency of Fe–S Cluster Biosynthetic Scaffold AtCnfU-V.” *Biochemical and Biophysical Research Communications* 340: 1047–1052. <https://doi.org/10.1016/j.bbrc.2005.12.104>.

Zannini, F., T. Roret, J. Przybyla-Toscano, T. Dhalleine, N. Rouhier, and J. Couturier. 2018. “Mitochondrial *Arabidopsis thaliana* TRXo Isoforms Bind an Iron–Sulfur Cluster and Reduce NFU Proteins In Vitro.” *Antioxidants* 7: 142. <https://doi.org/10.3390/antiox7100142>.

Supporting Information

Additional supporting information can be found online in the Supporting Information section.